Seminar series nr 123

Green roofs on municipal buildings in Lund - Modeling potential environmental benefits

Jacob Levallius

2005
Geobiosphere Science Centre
Physical Geography and Ecosystems Analysis
Lund University
Sölvegatan 12
S-223 62 Lund
Sweden

Green roofs on municipal buildings in Lund –

Modeling potential environmental benefits

Jacob Levallius

Supervisor
Harry Lankreijer

Master Degree Thesis
Department of Physical Geography and Ecosystem Analysis
Lund University, Sweden

2005

Abstract

Green roofs have the potential to mitigate problems with an urban heat island and to act as an element in stormwater management. Other environmental benefits exist as well, such as improvement of air quality, biological diversity and noise reduction. This project focuses on local community efforts to create a better environment through the use of extensive green roofs, which require almost no maintenance.

A sub area in Lund, Sweden, encompassing the University and University Hospital and with a high proportion of municipal buildings was simulated as having green roofs. The energy and water balances were modeled for two summer months. Storage heat changes were not analyzed.

85% of all municipal building areas, or almost 14% of the total area, were suitable as green roofs. Green space would increase from 42% to 55%. Runoff reduction for July and August were 22% and 58%, respectively. Daytime roof surface temperatures decreased 9° C on average. The increase in latent heat, also called evaporative cooling, and reduced surface temperatures brought a decrease in sensible heat and thus a potential mitigation of the urban heat island effect.

Other methods such as ponds and channels also serve to improve stormwater management but green roofs have the advantage of using free space and cool buildings at the same time. Applying green roofs on existing buildings is not very common, but this study shows that doing so on large roof areas can be beneficial to the local environment.

Keywords: green roofs, urban heat island, stormwater management, BMPs, Lund, environment, GIS

Sammanfattning

Gröna tak kan minska problem med s.k. urban heat islands och kan användas för dagvattenhantering. Andra miljöfördelar som en förbättring av luftkvalitet, biodiversitet och bullerminskning finns också. Detta projekt fokuserar på lokala (kommunala) medel för att skapa en bättre miljö med extensiva gröna tak, vilka är nästan underhållsfria.

Ett delområde i Lund som inkluderar Universitetet och Universitetssjukhuset och har en hög andel offentliga byggnader har simulerats att ha gröna tak. Energi- och vattenbalansen har modellerats för två sommarmånader. Värmelagring i byggnader har inte studerats.

85 % av alla takytor på offentliga byggnader, eller nästan 14 % av områdets area, är lämpliga för gröna tak. Gröna ytor skulle öka från 42 % till 55 %. Avrinningen från taken minskade med 22 % för juli och 58 % för augusti. Medeltemperaturen på takytorna under dagtid minskade med 9°C. Ökningen av det latenta värmeflödet och minskningen av yttemperaturen förde med sig en minskning av sensibel värme och därmed en potentiell reducering av urban heat island.

Andra medel som t ex dammar och kanaler är också viktiga i dagvattenhantering men gröna tak använder fördelaktigt oanvända takytor och kyler samtidigt byggnader. Att anlägga gröna tak på existerande byggnader är inte vanligt men resultaten i denna studie visar att gröna tak på stora takytor kan gynna det lokala klimatet.

Nyckelord: gröna tak, urban heat island, dagvattenhantering, BMPs, Lund, miljö, GIS

Acknowledgements

I feel there is more need for sustainable development – using resources and energy in a way that provides society with its needs but at the same time safeguards the environment. While not being the only solution or an answer to all aspects of environmental living, green roofs have many benefits that act to match an urban area to a pre-developed one. I thought it would be appropriate for me as a physical geographer with expertise in GIS and knowledge in the balance of energy and water to model these balances for green roofs.

Gratitude is expressed to Harry Lankreijer for supervising me and providing guidance along the way and to Johan Thiberg, my contact at Veg Tech, for his ideas and expertise on green roofs.

Further thanks to Louise Lundberg at the botanical garden of Augustenborg, Alla Yurova and Alexander Sedletski at INES, Karin Larsson at the GIS Centre and Thomas Åkerholm & Pethra Rosenlind at the Lund technical administration.

I would also like to thank my family for support throughout my higher education. Linda pitched the idea for this master thesis and her support has been invaluable. A thank you goes to Marta for introducing me to green roofs.

Finally, I would like to thank the Swedish Association of Graduate Engineers (Civilingenjörsförbundet) for financial support through the Environmental Scholarship Fund (Miljöfonden).

Table of contents

Symbols

	Description	Value/unit
T_a	Atmospheric temperature	C/K
T_s	Surface temperature	C/K
R_{net}	Measured net solar radiation	W m^{-2}
$K\downarrow$	Shortwave radiation in	W m^{-2}
$K\uparrow$	Shortwave radiation out	W m^{-2}
K^*	Shortwave radiation net	W m^{-2}
$L\downarrow$	Longwave radiation in	W m^{-2}
$L\downarrow_0$	Longwave radiation in, cloudless sky	W m^{-2}
$L\uparrow$	Longwave radiation out	W m^{-2}
L^*	Longwave radiation net	W m^{-2}
Q_H	Sensible heat	W m^{-2}
Q_E	Latent heat	W m^{-2}
Q_S	Storage heat flux	W m^{-2}
Q^*	Net radiation	W m^{-2}
S_B	Solar beam/direct radiation	W m^{-2}
S_D	Solar diffuse radiation	W m^{-2}
I	Precipitation intensity	mm hr^{-1}
P	Precipitation	
R	Runoff	
E_s	Solar constant	1367 W m^{-2}
E	Evapotranspiration	
m	Optical air mass number	
h_c	Convection coefficient	12
c_f	Cloud cover coefficient	%
w_a	Available water	%

Greek

α	Albedo	
β	Roof slope	Degrees
φ_S, φ_R	Solar azimuth, roof aspect	Degrees
ε	Emissivity	
ε_a	Emissivity of atmosphere	
θ	Sun radiation angle	Degrees
ψ	Solar zenith angle	Degrees
τ	Transmissivity of atmosphere	
λ	Latent heat of vaporization	2.44 MJ kg^{-1} K^{-1}
σ	Stephan-Boltzmann constant	5.67 E^{-8}

Introduction

1.1 Background

The denser a city is with buildings, industries and people, the more environmental challenges it faces. Many of today's urban cities are crowded with buildings, people and traffic and many areas are paved. Some negative impacts of this are increased urban temperatures compared to rural areas and more likelihood of flooding. These and many other problems can be mitigated by environmental planning and building techniques, such as improved housing insulation and stormwater management. In addition, potential future climate changes may further increase the need for ecological buildings.

The city of Lund, Sweden, has an area with a high concentration of municipal buildings – the area covered by the University and University Hospital. For this area, the city of Lund declared in 1998 that "a local handling of stormwater or, alternatively, detention dams, should be created in as large a scope as possible" and that "a careful treatment of ground, water and vegetation…will contribute to giving the area an attractive outdoor environment" (Miljöstrategiska enheten, 2002). Green roofs have the benefit of using free roof areas for addressing these issues and to potentially solve the urban problems mentioned earlier. Extensive green roofs can be applied to almost any building and require no watering or cutting.

1.2 Purpose

Most of the research to date on green roofs has focused on reducing the urban heat island effect and minimizing stormwater runoff, but few studies have combined these two or modeled the potential effects of green roof on a particular area. The intent of this study is to theoretically apply green roofs to municipal buildings and simulate potential environmental effects. Municipal buildings are chosen since the municipality is responsible for stormwater management on a broader scale and has the ability to stimulate environmental planning. Since buildings in Sweden generally are well insulated, focus is made on outside climate impacts rather than in-house. In more detail, the purpose of this study can be specified with three points:

1) To create a model for the hydrological and energy balance impacts of green roofs on specific existing buildings.

2) To use the model on municipal buildings in an area in Lund to study the potential environmental effects.

3) To provide information about all aspects of green roofs, demonstrate potential benefits and discuss the ability to use the model on other areas.

Simulating the environmental impacts will be done by modeling the water and energy balance of selected roofs with and without the use of extensive green roofs. A geographical information system[1] (GIS) will be used to extract roofs from digital maps of the area. Some field studies will be required for finding roof properties such as slope and material. After the creation of a model simulations will be performed based on measured climate data from a summer period.

The problems of urban development on the environment will be discussed in the first chapter, followed by comprehensive information on green roofs in chapter two. Then the study area will be described with a look at the local municipality and environmental policies. The last part of the report describes the method and developed model with results and a discussion on the simulations made.

[1] A representation of geographical features in a digital map with complex processing and visualization tools.

2 Urban problems

2.1 Runoff

Urban areas have many hard impervious surfaces such as roofs, streets and parking lots. Rain falling on these surfaces is called stormwater and is diverted to drains that connect to the city sewer system. Buildings, in turn, generate a lot of wastewater and traditionally this has been collected together with stormwater in a combined sewer. During an intense rain combined wastewater and stormwater can exceed the capacity of the collection system and cause polluted water to surface in what is called a combined sewer overflow (CSO). As part of a Best Management Practice (BMP), separated stormwater and wastewater piping is becoming more and more common. The benefits from these, in addition to preventing CSOs, are that the stormwater is not mixed with the wastewater and thus does not have to go through expensive treatment before being discharged to a recipient, usually a river or lake (Grozeva, 1997). In Sweden approximately 20-25% of the sewer network is of the older combined type (Villarreal, 2005).

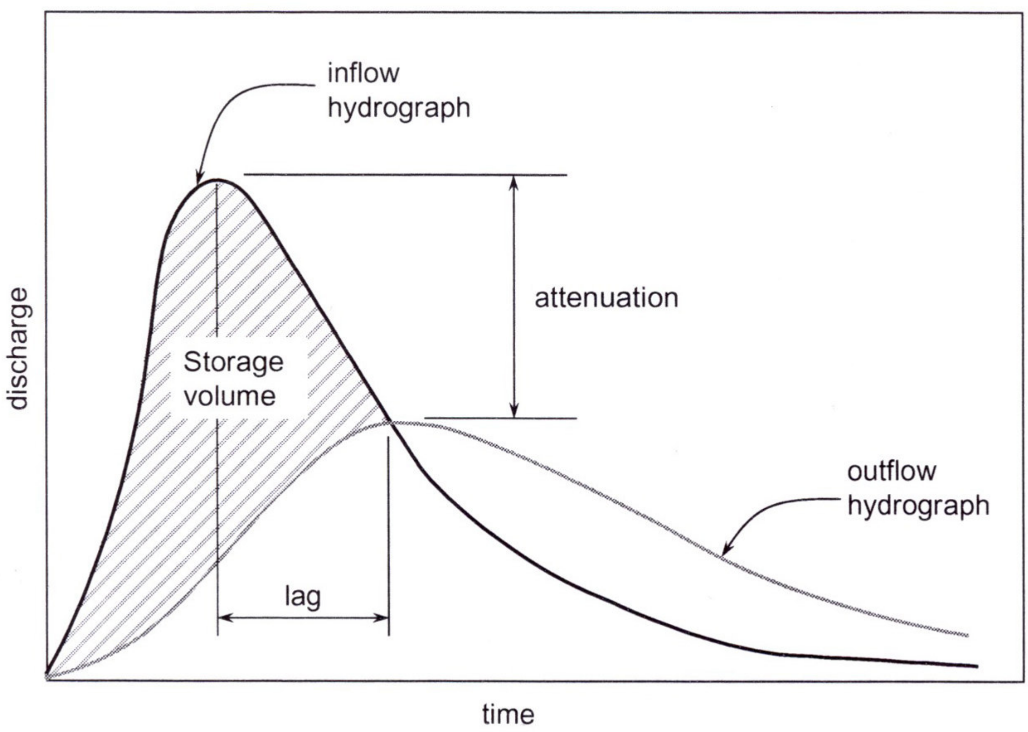

Figure 1. Stormwater retention (lag) and attenuation (peak reduction) with the use of BMPs. Source: Villarreal, 2004.

Other BMPs are the construction of ponds, detention systems of various types and a replacement of impervious surfaces such as asphalt and roofs with other materials. Applying green roofs is another BMP. These practices help to mitigate floods, which are a common problem in urban areas (Villarreal, 2005). The intent is to delay parts of the runoff (also known as discharge) in order to minimize the peak runoff, as seen in Figure 1. This way the total runoff is also reduced since water is collected in ponds and channels where it can evaporate. Some stormwater management methods are displayed further in Figure 5.

2.2 Urban heat island

Paved areas, streets and buildings overall reflect less solar radiation than natural surfaces such as grass and trees (Oke, 1987). The additional absorbed radiation on these hard and dry surfaces is transferred into energy and leads to an increase in surface temperature, which in turn increases the ambient temperature. Some energy may be used for evaporation if water is available on the surface. Anthropogenic processes such as waste heat from industries, air conditioners and the heating of buildings can add further warming to the city. European city temperatures have increased more than overall temperatures and the increase is most prominent during nights and winter (Haughton & Hunter, 1994). This effect is called an urban heat island and it has become a major problem in many low- and mid-latitude metropolitan areas (Taha, 1997; Bretz *et al.*, 1998). Figure 2 shows the urban heat island effect with a gradient of midnight temperatures in Singapore. Consequences of these are increased energy usage due to more need of air conditioners and increased smog. Akbari *et al.* (2001) found electricity consumption in six large American cities rising by 2-4% for each 1° C rise in daily maximum temperature above a certain threshold.

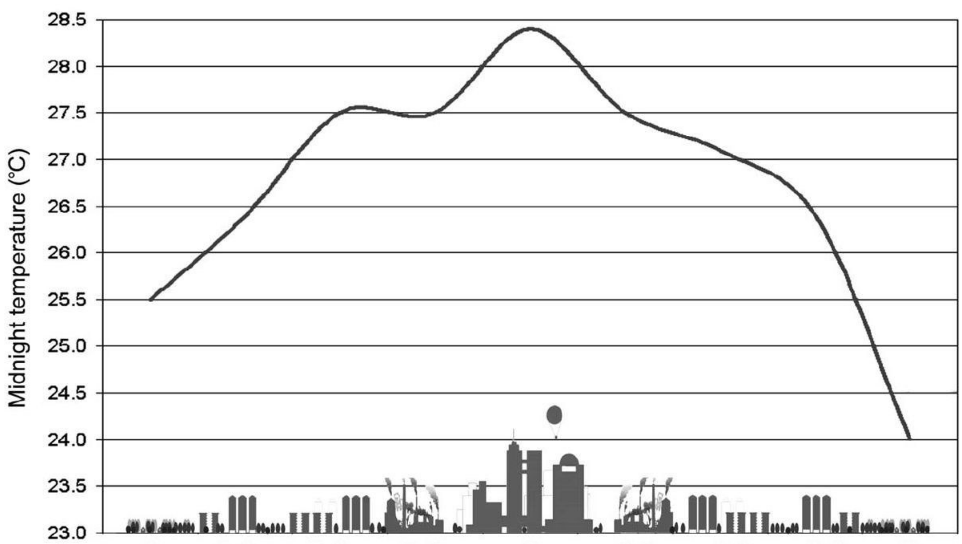

Figure 2. The urban heat island effect – Singapore midnight temperatures. The x-axis represents a line through the city and the shows that the highest temperatures are found in the city centre. Source: Wong & Yu, 2005.

Many cities have adopted techniques to reflect more of the sun's energy, mostly through the use of cool roofs. These use a high albedo, or solar reflectivity, to reflect more of the incoming radiation. Examples are white roofs or special roof coatings. Although this has helped to prevent high temperatures (Prado & Ferreira, 2005), it is still not an ultimate solution for a better city climate since it does not prevent dry air and may cause glare to surrounding buildings.

Roofs are just a small part of the urban surface. Many surfaces, especially in high-rise cities, are vertical. Some research on urban radiation is focused on urban canyons. These are spaces between buildings where radiation is trapped. The result is higher overall temperatures and smaller temperature variation than at the top of the buildings (Christen & Vogt, 2004).

Construction standards in Sweden are high and buildings are well insulated due to cold winters, which means that problems with high in-house temperatures are not particularly common. Nevertheless, potential warming may increase the need of cooling in summer (IPCC, 2001). In addition, even minor heat loss from buildings in winter can cause snow on roofs to melt, thus not taking advantage of the added insulation snow provides.

2.3 Other problems

Few buildings are ecologically constructed to the extent of what is capable with today's techniques and this largely depends on high initial costs, but also lack of awareness about solutions or benefits from these. Using energy efficiently is often not a concern to many people because it is usually not a large expense or the energy is paid for indirectly.

Crowded cities also face problems with noise from traffic and this is enhanced with additional hard surfaces that reflect noise. Grass, plants and trees absorb noise instead. The construction of urban areas not only replaces a biological green space but also acts as a disturbance to many plants and animals. Many city areas have expanded in a high pace and people are moved further and further away from green areas. Pollution from cars and factories are a significant problem, especially in combination with an urban heat island, which traps pollution within the city and can cause health issues. Dry air is another product of removing permeable land and further enhances problems with pollution. Large temperature differences on rooftop surfaces and exposure to ultraviolet radiation can shorten the life of a roof membrane considerably.

3 Green roofs

3.1 History

The general definition of green roofs are roofs with vegetation. One of the most famous early examples of green roofs is the Hanging Gardens of Babylon, which is one of the Seven Wonders of the World. Traditionally sod (also called turf) roofs have been used in Scandinavia as an anti-fire protective measure by covering the roof with fire resistant soil. Grass develops over time to create a sod roof (Grozeva, 1997). Modern green roofs were first used in Switzerland in the 1960s as stormwater management and spread to Germany in the late 1970s. Today they are broadly used and are, in some parts, required by law as a means to preserve a certain degree of green space (www.gnla.ca). Green roofs are most widely used in Germany, where approximately 14% of all flat roofs are green (VanWoert *et al*., 2005).

The first modern green roofs in Sweden arrived in the early 1990s and have only become commonly used in occasional projects or as part of new housing areas with an environmental profile, such as the West harbor (Västra hamnen) in Malmö in 2001. Green roofs also occur in some places in Lund as described in chapter 4.

3.2 Types

There are two types of green roofs: intensive and extensive. Intensive green roofs can be a few decimeters thick and can grow flowers, bushes and even small trees (Figure 3b). This type of vegetation is heavy and is often not applicable to a normal roof without reinforcing it and also needs to be watered and frequently maintained. Extensive roofs are used for this study and are only a few centimeters thick with moss-sedum or sedum-herb vegetation (Figure 3a). Long periods without rain has no permanent effect on these drought-tolerant species and thus extensive green roofs do not need to be watered, nor cut. The appearance of extensive green roofs vary throughout the season and maintenance is low, which will be described later on. Henceforth green roofs refer to extensive green roofs.

Figure 3. Extensive (a) and intensive (b) green roofs. Source: Veg Tech.

3.3 Environmental benefits

Some of the major current global environmental concerns are biodiversity, climate and pollution (Haughton & Hunter, 1994). Green roofs have been successful in addressing these and many other environmental problems, which will all be described more in detail:

- Stormwater management
- Urban heat island and air quality
- Biodiversity
- Protection of roof membrane
- Noise
- Aesthetics

3.3.1 Stormwater management

Green roofs have the ability to store rainwater and thus help delay peak flooding and reduce runoff volume. Bengtsson (2002) studied the monthly and annual water balance for a green roof and found that about half of the yearly precipitation (368/719 mm) became runoff. In general, runoff exceeded the evapotranspiration from August to February but was less from March through July. Some of the winter precipitation was snow, which does not create instant runoff, and August and September had the highest precipitation, 89 mm and 124 mm respectively. Even if the substrate is filled to capacity, it takes some time for the water to flow vertically through it and Bengtsson (2002) found this delay to be about 20 minutes. For designers of stormwater systems green roofs can thus be beneficial in delaying runoff and lowering peak flows. Green roofs with a 3 cm dry substrate and a 1.5 degree slope has the ability to retain about 10 mm rain before runoff is initiated (Villarreal, 2004). If the substrate is not initially dry less water is needed to initiate runoff and once the substrate is at field capacity the runoff is likely to be the same as the rain intensity. The evapotranspiration from green roofs will be highest when rain showers are followed by dry periods. If green roofs were to be used in equatorial countries with long rain periods followed by long dry periods, the evapotranspiration would be very small. Therefore the best application of green roofs is in climates without a rain season. Ponds and channels are a way to further increase capacity when green roofs are insufficient.

Measurements on green roofs in Berlin in 1987-1989 found that only 20.9-26.4% of the annual precipitation became runoff, with cooling benefits of between 252 and 356 kWh m^{-2} per year (Koehler *et al*, 2001). A 14-month field study by VanWoert *et al.* (2005) showed very high retention for light rains (96.2%) and a significant 52.4% of heavy rains. The overall retention for 556 mm rainfall was 60.6%. The rate of runoff is by VanWoert *et al.* described as a bigger problem than runoff volume due to treatment capacity.

The quality of the runoff water from extensive green roofs has been studied by Berndtsson *et al.* (2005). Green roof waters were found to have higher concentrations of contaminants, with the exception of nitrogen. This is partly attributable to fertilization during establishment, after which green roofs show considerable amounts of phosphate in runoff. Therefore easily dissolvable fertilizers should be avoided. Berndtsson emphasizes that even though green roofs are not recommended for rain water treatment, they have many other positive functions in the urban environment.

3.3.2 Urban Heat Island mitigation

Green roofs have a lower solar reflectivity than the materials used for cools roofs but they store rainwater and generate heat loss through evapotranspiration. As described earlier, the cooling benefits from evapotranspiration can be high. In addition, energy is saved through increased insulation with a green roof, which works both in winter and summer and can reduce energy use for air conditioning (Grozeva, 1997).

Wong & Yu (2005) found significant differences between midnight air temperatures in the outer edges of Singapore compared to the city centre (Figure 2). The largest difference was 4° C and the higher temperatures had a negative impact on humidity, creating a drier climate in the city centre. Reducing the urban heat island effect and thereby increasing humidity has a positive effect on the quality of the air (Akbari *et al.*, 2001).

3.3.3 Other environmental benefits

Green roofs have also shown potential to mitigate noise, filter pollution and provide a richer biological diversity. Less measurable but equally important are the possible health benefits from a green environment and its aesthetics. A study by Ulrich (2000) shows patients in hospitals recovering faster with access to or room view into a green environment. When roofs available to support it, intensive green roofs can also act as a roof garden where patients can stroll. Another use of roof areas is solar panels and green roofs have the ability to increase the performance of the solar cells by lowering the ambient temperature (Lundberg, personal communication).

Green roofs are common on many European airports where they, in addition to previously mentioned advantages, help to reduce birds around the runways. These hazardous birds like hotter sterile roofs better than green roofs and also like ponds (Velasquez, 2005). The use of green roofs reduces runoff and the need for ponds that attract birds.

3.4 Economic benefits

Increased insulation decreases energy costs for the buildings and for hot time periods this can lead to reduced air conditioning usage, lowering energy costs. Daily variations in temperature cause wearing of the roof membrane through expansion and shrinkage and ultraviolet radiation damages the roof further. Extensive green roofs have a lower life-cycle cost than standard roofs and this is enhanced further when considering energy savings (Wong *et al.*, 2003). Many areas in Germany use green roofs to benefit from reduced stormwater fees (www.gnla.ca). Other benefits are not easily measured, such as therapeutic value and increased biodiversity. A greener city creates allows for more buildings on a smaller space.

3.5 Detailed description

Green roofs are generally composed of a vegetation layer, a substrate layer and a drainage layer (Figure 4). There is often a filter between the substrate and the drainage layer in order to prevent fine particles in the soil substrate from washing out. The substrate layer is composed of soil and inorganic materials with low density and a high water-holding capacity such as crushed brick, expanded clay, lava rock or pumice. Often the location and the slope of the roof determine which material mix is most suitable, but water retaining ability, preference, cost and aesthetics also play a role (Veg Tech).

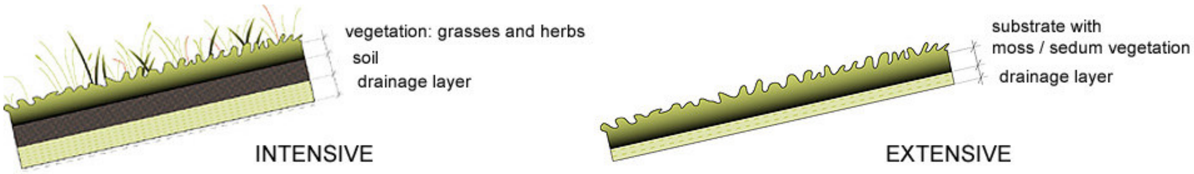

Figure 4. Typical buildup of a green roof. Intensive and extensive are similar, but intensive have other types of vegetation. They also require a roof that can hold more weight since they need more storage of water and thus have thicker layers. Source: Veg Tech.

The purpose of the drainage layer is to avoid permanent water on flat areas of flat or low-sloped roofs, since this encourages weed growth. It also serves as a water reserve for the vegetation. On extensive roofs the drainage layer is no more than a couple of centimeters thick, whereas on intensive roofs the layer can be more than a decimeter thick.

3.6 Requirements

The Swedish green roof market offers prefabricated green roof mats, which is the most common way of constructing green roofs in Sweden. It also offers on-site planting of sedum cuttings, which is more used in Germany (Emilsson & Rolf, 2005). Flat or low sloping roofs offer the ability for this low cost solution of on-site establishment, but according to Emilsson & Rolf it requires somewhat more maintenance during the initial phase and takes a few years to reach full plant cover. In addition, heavy rains or stormy winds may cause problems before vegetation has started to grow. Extensive green roofs need to be fertilized during the first two years, after which it is normally not needed. Regular checkups every year or so on the vegetation and gutters should be performed to insure a well functioning green roof.

Several types of green roofs exist with differences in substrate and plant species. This study uses *Veg Tech Xeroflor Moss-sedum*, which has a 3 cm substrate. Stems may reach over a decimeter in height during summer flowering. Green roofs require a weather resistant roof membrane, which all bituminous and PVC single ply membrane roofs have. Experiments at the botanical garden of Augustenborg in Malmoe show that constructing green roofs directly on tile roofing is possible as well, although this is not recommended. Tile roofs are preferably removed and replaced with an ordinary smooth roof membrane, on top of which green roofs can be constructed. The maximum weight of the total construction saturated with water is 50 kg m^{-2} and this should never exceed the capacity of a normal roof. Intensive green roofs are heavier and add 130 kg m^{-2} to the roof weight. Usually a truck with a crane is used to transport green roof material to the roof during construction. Tall buildings may require a separate larger crane.

Fire is not a problem with green roofs since the moss-sedum vegetation used for this study is fire protection approved. This is accomplished by a large share of inorganic content in combination with high water levels in the vegetation.

3.7 Green roof usage

Once unused roof areas have been turned green, complimentary steps should be taken for additional effect. Intensive green roofs can hold even more water than extensive and can be built as a rooftop garden. Vegetation as facing on a building can increase the insulation of a building and enhance the green environment. Runoff water from green roofs can be collected and used for watering, or can be stored for buildings' use of washing and flushing. Runoff from other impervious areas should be channeled to ponds or swales. Materials such as gravel, permeable asphalt and permeable concrete can replace impervious surfaces (Stahre, 2004). Rasterized hard plastic can be used on parking areas for percolation of rain water and thus a decrease of impervious surfaces. Figure 5 shows how these and other techniques can be used.

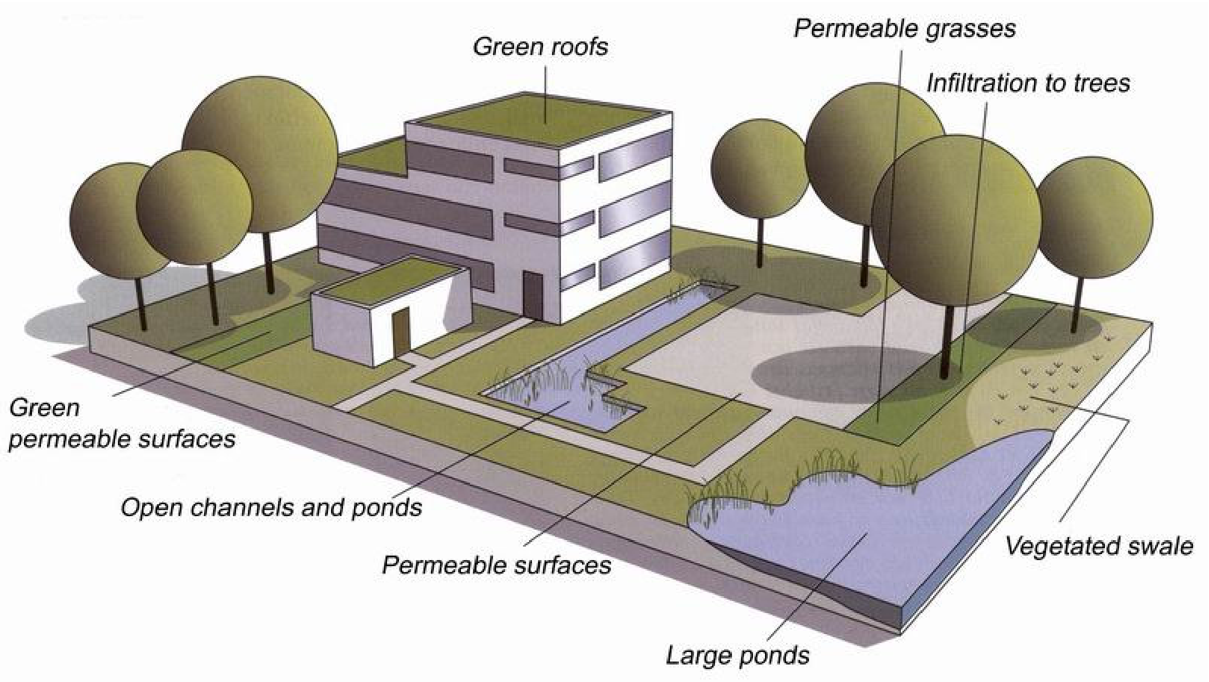

Figure 5. Urban stormwater management. Source: Veg Tech.

The most significant drawback of a green roof is the high initial cost of construction, but as mentioned earlier this cost will in the long run be compensated for in more ways than what is measurable. A potential negative effect may be dissolution of fertilizers into runoff water. Water leakage or similar issues should not be a problem if the roof is appropriately constructed.

3.8 Green roofs on municipal buildings

Germany is where green roofs are most common and also where greening policies are most widely used. Goya (www.gnla.ca) outlines existing policies very well and also gives advice on considerations for new greening policies. Some cities are required to apply green roofs to flat public buildings. In general the existing policies are:

1. direct and indirect financial incentives
2. ecological compensation measure
3. integration into development regulation

No such green policy on environmental building exists yet for Sweden. The Unites States Green Building Council (USGBC) has developed a standard for environmental construction. It gives project developers the ability to certify a building as having a certain degree of sustainability. The Leadership in Energy and Environmental Design (LEED) certification was created to (www.usgbc.org):

- define "green building" by establishing a common standard of measurement
- promote integrated, whole-building design practices
- recognize environmental leadership in the building industry
- stimulate green competition
- raise consumer awareness of green building benefits
- transform the building market

Municipalities are increasingly using this new certification on new and existing municipal facilities. As of May, 2005, 41 city and county governments had to some degree adopted LEED as a requirement in construction or renovation of municipal buildings (Suttell, 2005). LEED offers four different ratings: certified and silver-, gold- or platinum certified, where silver is the most common requirement. Chicago has a LEED silver requirement on all new city-funded buildings and major renovations and is becoming known as a green city. The large city hall green roof has native trees and even beehives. Setting a size limit over which projects are forced to follow LEED is also common, as in Seattle where city projects larger than 5,000 square feet (~465 m^2) have to meet LEED silver certification. Scottsdale, AZ, and Vancouver have a gold requirement on new public buildings (Suttell, 2005).

4 Study area

4.1 Lund overview

Lund is a very old city with about 100,000 inhabitants. Today it is mostly associated with the large University with about 40,000 students and 6,000 faculty and staff and the University Hospital with 8,000 employees. The university includes a technical university, called Lunds Tekniska Högskola (LTH). Some important companies are Alfa Laval, Astra Zeneca, Sony Ericsson and the headquarters of Tetra Pak.

Green recreation areas are fewer in Lund (63 m^2/inhabitant) than the average for the ten largest communities in Sweden (108 m^2/inhabitant). 23% of urban areas in the Lund community are impervious areas (Lindegren, 2002). Some green roofs already exist in Lund. The Gunnesbo school from 1994 has one of the oldest constructed modern green roofs in Sweden (about 1000 m^2). A housing complex called Klostervallen was finished in 2003 and has about 3000 m^2 green roofs, in addition to the rare use of district cooling.

For the city as a whole, about 20% of all stormwater is collected in an inferior combined sewer system (Miljöstrategiska enheten, 2002) and the rest through separate sewer and stormwater pipes in a Best Management Practice (BMP) fashion. An estimated 15-20% of stormwater is detained through ponds (Miljöstrategiska enheten, 2002). The recipient of stormwater and treated sewer water is Höje river in the south outskirts of Lund, where the treatment plant is located (Figure 6:A).

4.2 Study area overview

The study area is located close to the center of the city and occupies about 1.4 million m^2, or 140 hectares. It is heavily dominated by the University, especially LTH, and the University Hospital as shown in Figure 6. High technology companies in the Ideon park occupy some of the easternmost areas (white roofs in photo) while some private housing occurs in the southern parts. The area is not significantly dense with buildings, but a majority of the buildings are municipal, which are the ones considered for green roofs. Lund slopes to the southeast towards the Höje river (A) and the study area is situated the highest in Lund, causing stormwater to flow through the pipes under the rest of the city before reaching the treatment plant or recipient. There is a 20 m difference in study area elevation from the lowest level in the southwest to the highest in the northeast (55-75 m). During the past decades the use of the area has grown substantially and new buildings are consistently added. In the last five years some large parking houses (B), an astronomy building (C) and a design building (D) have been added. This report uses the state of the buildings in October 2004, with the most recent addition being an extended Literature complex (E). The current reconstruction of the Chemical centre (Kemicentrum, F) is not considered. Figure 6 also gives some idea of the greenness in the area. Buildings are more visible in Figure 9 in the results.

In the study area separate pipes are most prominent, but combined systems are still used in an area directly south of the University Hospital. Few ponds exist in the area, but one is located on the campus of LTH. The major roads within the area are Tornavägen in a north-south direction and Sölvegatan in an east-west direction. One part of a road is restricted to bus traffic as part of the Lundalänk, which serves as a quick way of public transport from the city centre to the Hospital, LTH and Ideon.

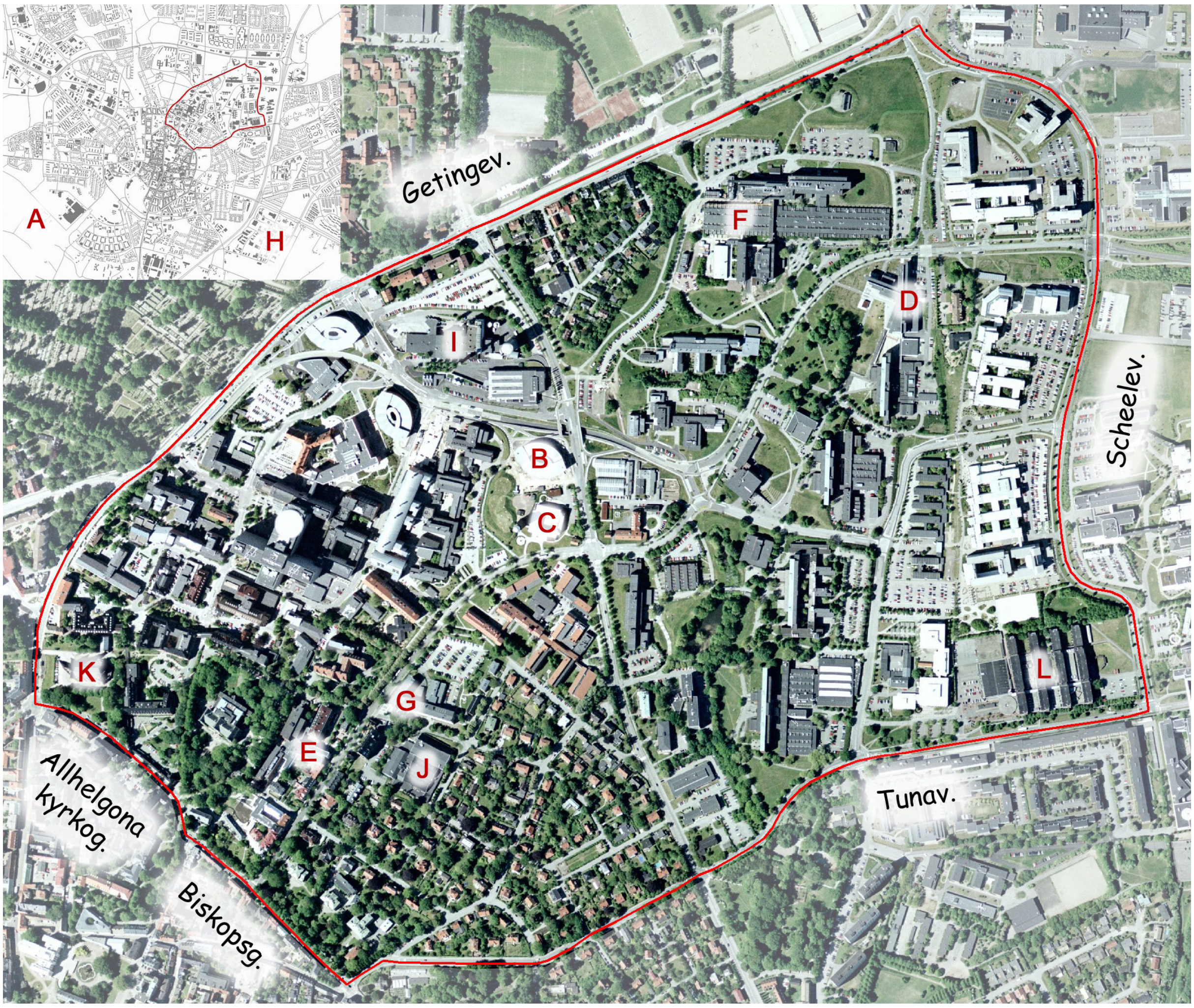

Figure 6. Orthophoto of the study area. The typed roads enclose the area, shown with a red line. Orthophoto: Lund technical administration.

The geographic location of the area is 55.716 N, 13.202 E. The weather station from which climate data is acquired is at altitude 60 m and is located on the rooftop of the department of Physical Geography and Ecosystems Analysis (G). Precipitation data is measured at the fire station in the south outskirts of Lund (H), roughly 2 km SSE from the study area and at about 30 m lower altitude.

4.2.1 Municipal Buildings

When considering the application of green roofs only municipal buildings are observed because this report focuses on local community efforts to create a better environment. This is also the reason for choosing this area in which municipal buildings cover about three quarters of all building space. These buildings are composed almost entirely of the University and the University Hospital. Among the exceptions are a power plant delivering energy to the Hospital (I), a large athletics and recreational facility (Gerdahallen, J), a church (Allhelgonakyrkan, K) and a student housing complex (Sparta, L).

4.3 Actors

4.3.1 Municipality of Lund

An "overview plan" (översiktsplan) is a document without legal bindings that outlines future plans for an area. Lund has set up guidelines that include aims to improve stormwater management, biodiversity and green structure. A more detailed analysis of the plan from 1998 was made on the study area in question and it has a few standpoints relevant to this study, such as the following (Stadsarkitektkontoret, 1998):

- "The vegetation is a valuable part of the city environment that can be enhanced further…"
- "A careful treatment of ground, water and vegetation…will contribute to giving the area an attractive outdoor environment."
- "A local handling of stormwater or, alternatively, detention dams, should be created in as large a scope as possible."
- "Separate calm outdoor environments shall be created for patients, visitors and for the recreation of employees."

4.3.2 Lund University and University Hospital

Lund University declared in 1998 that energy consumption would be cut 10% by 2006 and that the sewer volume transported to the city pipelines should be reduced by 5% by the same time (Stadsarkitektkontoret, 1998). The latter of these goals has already been achieved. The hospital buildings are almost exclusively owned by Malmöhus Läns Landsting.

4.3.3 Akademiska Hus

Many University buildings are owned by Akademiska Hus. They rent out 350,000 m^2 of office space in Lund, with the University as their biggest tenant. An installation of district heating (fjärrvärme) and cooling has been added to the Literature centre and one of the largest underground heat and cooling systems in Europe is currently being built for the LTH chemical centre, making this and nearby buildings that occupy more than 50,000 m^2 self-reliant on energy for heating and cooling. For the chemical centre there are 165 holes that run 230 m deep. Akademiska Hus has far-reaching environmental goals, was recently ISO 14001 certified and aims to reduce energy use 30% by 2025 (www.akademiskahus.se).

5 Method

5.1 Theoretical basis

The energy balance for a surface can easily be described as the energy that flows into and out from the surface. Solar radiation is the dominant source of energy to the surface and received energy is channeled into latent-, sensible and storage heat (Figure 7). Latent heat is the energy loss by evapotranspiration, which is a group term for evaporation of free water and transpiration of water in vegetation. Sensible heat is caused by the temperature difference between a surface or soil and the atmosphere. Storage heat is an increase in temperature of urban materials and ground surfaces, an energy which usually is released at night.

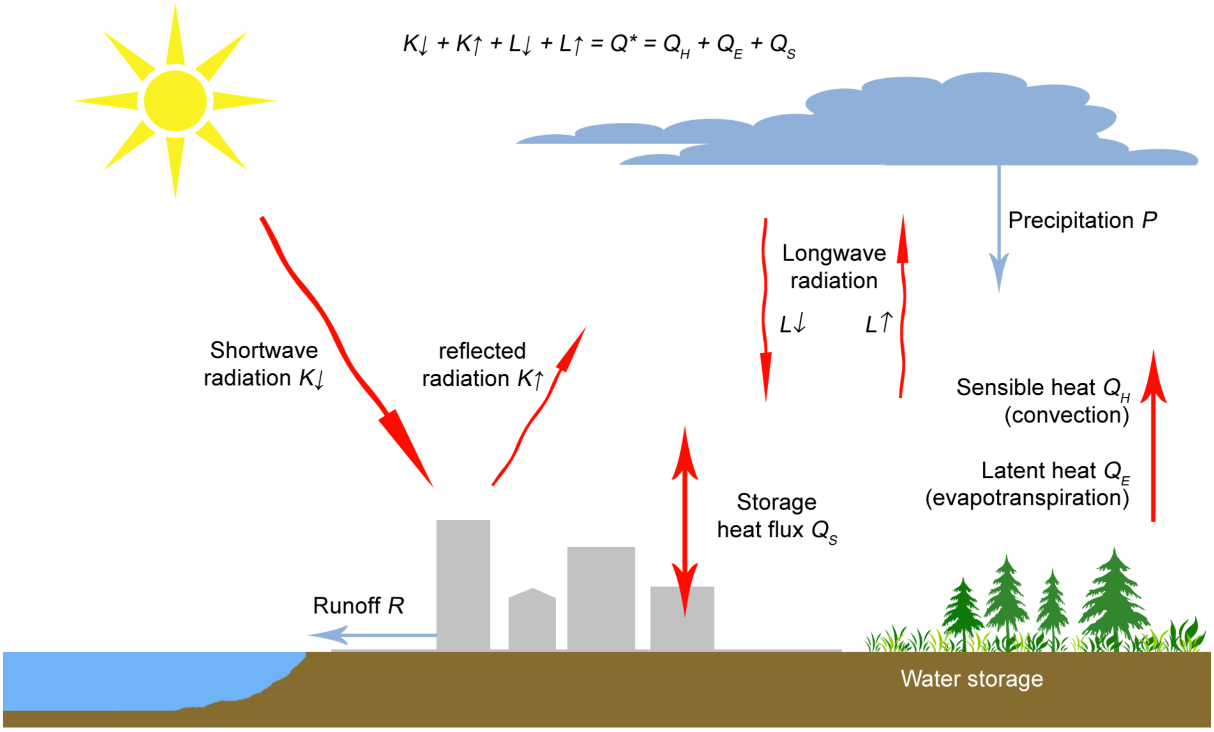

Figure 7. The water, radiation and energy balance of a surface. A body or surface emits radiation based on surface temperature. The sun emits shortwave radiation and $K\downarrow$ equals the radiation that is transmitted through the atmosphere as direct or diffuse shortwave radiation. The earth and atmosphere emit long wave radiation L. Sensible heat Q_H is energy transfer by convection due to wind. Evapotranspiration of water equals the energy Q_E. Storage heat flux Q_S causes a temperature increase or decrease. Sometimes a ground heat flux is used as the energy transfer between buildings and the ground (not shown). Water is stored or transferred to rivers and lakes.

Radiation is divided into longwave and shortwave. The sun emits visible shortwave radiation due to its surface temperature of about 6000° K. Surfaces with low temperatures, such as the earth, emit longwave radiation (L) that is not visible to the naked eye. Thus, shortwave radiation (K) occurs only when the sun is above the horizon, whereas L is diurnal. A surface reflects a certain amount of the sun's shortwave radiation, determined by a fraction called albedo. L is emitted to the earth's surface from the atmosphere, and this is increased by higher temperatures and clouds. The energy balance equation for a natural surface can be written as Eq. 1.

$$K\downarrow + K\uparrow + L\downarrow + L\uparrow = Q^{*} \quad (1)$$

The arrows in equation 1 show the direction of the radiation and Q^{*} is the net radiation. For our purposes the energy direction is from the surface point of view, which means that energy flowing to the surface is positive and a loss of energy is negative. Q^{*} is matched by other energy transfers for equilibrium to be achieved (Eq. 2).

$$Q^{*} + Q_H + Q_E + Q_S = 0 \quad (2)$$

Q_H and Q_E are sensible and latent heat, respectively. Q_S is the heat storage in the surface layer, in this case energy storage in the roof. For urban areas anthropogenic heating (Q_F) exists as well and this is discussed later on. For this model, the only measured radiation variable is incoming solar radiation on a plane surface. The most important variable to extract is the dynamic surface temperature (T_s) of the roof. For this, a series of calculations are performed to find input variables for the energy balance equation, from which T_s is found.

5.1.1 Solar radiation

Measured solar radiation for a flat surface is available, but since radiation on a roof will be different depending on its slope and direction, a rather complicated approach has to be made to find radiation on each roof. Radiation from the sun diminishes as it passes through the atmosphere and atmospheric conditions determine the transmissivity (τ) which can be described as the ratio of solar radiation that reaches the surface of the earth. Some radiation is scattered by the atmosphere before reaching the surface and thus solar radiation consists of direct (S_B) and diffuse (S_D) radiation. The measured solar radiation on a plane surface (R_{net}) will be used to extract τ using Campbell & Norman's (1998: pp.172-173) adaptation of Liu and Jordan, as seen in equation 3. R_{net} is set as equal to the sum (S_T) of S_B and S_D to find τ for each timestep.

$$R_{net} = S_T = S_B + S_D = S_P \cos\psi + 0.3\left(1 - \tau^{m}\right)E_S \cos\psi \quad (3)$$

$$S_P = E_S \tau^{m} \quad (4)$$

$$m = \frac{1}{\cos\psi} \quad (5)$$

ψ is the solar zenith angle for the time when the value was measured, found using an online application called MIDC SOLPOS Calculator (www.nrel.gov). The solar constant E_S is the solar irradiance per unit area and is set at 1367 W m^{-2}, which is the average value over a year (Wehrli, 1985). S_p is the irradiance below the atmosphere. Since the weather station is located

60 m height altitude effects are considered to be negligible and therefore the optical air mass number *m* does not include a correction for altitude.

The transmittance is used to find values for S_B and S_D but also a theoretical cloudiness or atmosphere clarity, which is then used to find $L\downarrow$. Gates (1980) suggest a value of $\tau_{max} \sim 0.75$ on the clearest days, which means that a cloudiness factor c_f can be calculated with Eq. 6.

$$c_f = 1 - (\tau / \tau_{\max}) \tag{6}$$

This method of extracting transmissivity from measured radiation works well during the day, but for the hours after sunrise and before sunset calculated τ is higher than the chosen τ_{max}. For these hours, τ is set to τ_{max}. A comparison between R_{net} and the corresponding calculated S_T show accumulative differences of less than 1‰.

The direction, or aspect, of the roof slope has significance for a northern latitude country like Sweden because the more slope a roof has the greater the difference in total radiation will be, due to the sun's low position. The solar beam angle of incidence (θ) to the roof is different for each timestep. It is calculated using the static slope (β) and aspect (φ_R) of the roof and the dynamic azimuth (φ_S) and zenith angle (ψ) of the sun (Eq. 7). This model uses north as the zero aspect of roofs and azimuth of the sun. A value for θ over 90 degrees means that there can be no direct (S_B) radiation to the surface, only diffuse (S_D).

$$\cos(\theta) = \cos(\beta)\cos(\psi) + \sin(\beta)\sin(\psi)\cos(\varphi_S - \varphi_R) \tag{7}$$

The final shortwave radiation received by a roof (Eq. 8) follows Lambert's cosine law (Oke, 1987).

$$K \downarrow = S_P \cos(\theta) \tag{8}$$

After an appropriate value for incoming solar radiation has been found, the amount that is reflected needs to be calculated. Albedo (α) for the different surfaces is difficult to know without measuring it in the field. In reality α changes with θ, but this difference is often rather small and occurs at the higher angles when the incoming radiation is low, thus minimizing the potential errors. Generally α will change more for a smooth surface than for a granular one. Weathering over time by ultraviolet radiation and buildup of pollution and biological growth causes the reflection properties to change. This aged albedo creates a decrease for high albedo surfaces. Since there are a variety of different surfaces, an approach was made to find appropriate aged albedo values for each typical surface (Table 1). Roof types were divided into eleven classes, where the eleventh was classified as *other* and was not included in the calculations. Table 1 also shows emissivity values, which are described below with longwave radiation.

Table 1. Radiation properties of used materials.

Material	**Albedo** (α)	**Emissivity** (ε)	**Reference**
bituminous	0.15	0.90	Bretz (1998), Parker (2000)
tile light	0.25	0.90	Bretz (1998), Levinson (2005)
tile dark	0.15	0.90	Oke (1987)
metal white	0.60	0.90	Parker (2000), Prado (2005)
metal grey	0.30	0.60	Parker (2000), Prado (2005)
metal black	0.10	0.90	Oke (1987), Parker (2000)
metal green	0.25	0.25	Oke (1987), Parker (2000), Prado (2005)
green roof	0.25	0.95	Oke (1987)
concrete	0.30	0.90	Oke (1987), Prado (2005)
glass	0.10	0.90	Oke (1987)

Finally, net shortwave radiation is calculated with equation 9.

$$K^* = K\downarrow + K\uparrow = K\downarrow (1-\alpha) \quad (9)$$

5.1.2 Longwave radiation

Outgoing longwave radiation is normally larger than the incoming, which means that net longwave radiation (L^*) is usually negative. On a clear day the incoming longwave radiation will be lower than on a cloudy day. Clouds are good emitters and will absorb, reflect and emit radiation back to earth. Typical values range between 230 and 380 W m^{-2} (Monteith & Unsworth, 1990: p.54). The incoming longwave radiation can most accurately be calculated using Eq. 10. $L\downarrow$ will also increase with smog and pollution over the city.

$$L\downarrow = \varepsilon_a \sigma T_a^4 \quad (10)$$

Since the emissivity (ε_a) is not easily known, $L\downarrow$ for a cloudless sky can be estimated using a linear function (Eq. 11) from Monteith & Unsworth (1990: p 52).

$$L\downarrow_0 = c + d\sigma T_a^4 \quad (11)$$

Constants c and d are 213 and 5.5, respectively. This formula does not include cloud effects, and even though nighttime cloudiness cannot be determined in this model an attempt is made to include cloud effects during the day (Eq. 12), using Oke (1987: p. 373).

$$L\downarrow = L\downarrow_0 \left(1 + ac_f^2\right) \quad (12)$$

Variable a depends on the type of cloud and since this is not known an average value of 0.2 is chosen (Oke, 1987: table A2.3). Cloud cover is extracted from calculated τ, but these values are only available for daytime hours. The average daytime τ for the whole current month is therefore used as a basis for nighttime cloudiness. In this model, $L\downarrow$ calculations are most accurate under average atmospheric conditions and are therefore not suitable for diurnal analysis.

Longwave radiation from the surface is determined by the surface temperature (T_s) and the emissivity (ε). Thus, $L\uparrow$ is calculated after the surface temperature has been determined, as seen in equation 13. Typical values range from -270 to -430 W m^{-2} (Monteith & Unsworth, 1990). Emissivity values are presented in Table 1. Green and grey metal categories include copper, painted or unpainted aluminum and galvanized tin. Metals without a coating or paint have a very low emissivity, which significantly alters the radiation balance compared with a high emissivity. Grey metal roofs in the area are assumed to exist both with and without a coating and therefore a mean value is estimated. An ε value of 1 corresponds to a blackbody, which means that given a certain surface temperature, the outgoing longwave radiation will be as high as possible. Most natural surfaces have an emissivity between 0.9 and 1.0. Roofs and other unnatural surfaces reach higher surface temperatures than evaporative surfaces and will have higher values of $L\uparrow$ during sunny daytime hours. Metals with low emissivity are an exception and lead to low $L\uparrow$ values and a negative L^*.

$$L\uparrow = \varepsilon\sigma T_s^{4} \tag{13}$$

5.1.3 Sensible heat

Sensible heat (Q_H) is decided by the temperature difference of the surface and the atmosphere and convection by the vertical wind component. The latter is not known and therefore Q_H is calculated with a constant value for convection, as shown in equation 14. The chosen value for convection coefficient (h_c = 12 W m^{-2} K^{-1}) is from moderate-wind standard conditions specified by ASTM 1980-98 (Prado, 2005).

$$Q_H = h_c(T_s - T_a) \tag{14}$$

Differences between the sensible and latent heat are often compared using the Bowen ratio, which is Q_H/Q_E. A high value implies a dry surface and typical urban values are 2-5, while rural areas have values below 1 (Christen & Vogt, 2004).

5.1.4 Heat storage flux

Energy is stored in buildings during the day and is released at night. At daytime there will be a larger storage in urban areas than in rural and, consequently, a larger release at night. The storage heat exchange (Q_S) depends on the surface temperature as well as the thickness and physical properties of interior roof materials. The latter properties are not easily known and thus Q_S is difficult to calculate. Nevertheless, a storage heat exchange is needed in the model to avoid exaggerated surface temperatures. Therefore a value is chosen as a ratio of the net radiation. Roofs generally have less mass than the walls of a building and walls will therefore store almost as much as the roof. Studies suggest the ratio of Q_S/Q^* for total heat storage to be -0.27 (Offerle *et al.*, 2005). Heat storage in roofs is thought to be roughly half of the total storage and therefore a ratio of -0.15 is chosen. Nighttime Q_H and Q_E values are usually close to zero. This is preferred in the model and the zero values are achieved by setting the Q_S/Q^* to -1.0.

$$Q_S = -0.15Q^* \text{ when } Q^* > 0 \tag{15}$$
$$Q_S = -Q^* \text{ when } Q^* < 0$$

Buildings store heat in the roof layer and also transmit heat into the building. Both these factors are considered to be included in the Q_S/Q^* ratio. Green roofs act to increase insulation and decrease surface temperatures, both of which has a negative effect on heat storage. Lundstedt & Karlsson (2003) show that the transmission of heat into a building is reduced by the use of green roofs. However, the insulation reduction on Q_S for moderate to well insulated roofs, which are a norm for Sweden, is quite small (Niachou *et al.*, 2001). Storage into the building usually peak before midday and release of energy starts between one and three hours before the net radiation becomes negative (Christen & Vogt, 2004). In this simplified model that will not be the case and so the use of Q_S to compensate high surface temperatures will give lower surface temperatures during the last hours of the day than will be likely in the field.

5.1.5 Anthropogenic heat

Urban areas use large amounts of energy for heating but this is most prominent in winter. Heat is also a byproduct of industrial processes, cars, etc., and this should be included in an energy balance equation. Without taking into account time, urban values are typically around 20 W m^{-2} (Christen & Vogt, 2004). In most major US cities, the value ranges from 20-40 in summer to 70-210 in winter for city centers (Taha, 1997). Offerle *et al.* (2005) showed that for a city in Poland the summertime (June – August) anthropogenic heat flux was -3 W m^{-2}, so for this model, which is used for summer months in a relatively small city, the anthropogenic forcing is considered negligible since almost no heating occurs in summer and because finding an appropriate value would be time consuming. The green roof effects on insulation, however, argue towards less Q_F for buildings covered with green roofs.

5.1.6 Water balance

The water balance for the green roof surface consists of input from precipitation, storage in the substrate and ouput by evapotranspiration or runoff. Field capacity is a measure of how much water the substrate can hold under the influence of gravitation. In this model field capacity includes storage in the drainage layer. Water level is a measure of the amount of water present in the green roof as a percentage of field capacity. This model simplifies the water balance by using a bucket approach in which precipitation will not create runoff until the field capacity has been reached.

5.1.7 Evapotranspiration

Latent heat release (Q_E) equals the amount of energy needed for evapotranspiration (E) at a certain temperature. A method to calculate Q_E directly is tested using a relationship based on the known variable relative humidity (h_r) and calculated K^*. This formula calculates the potential evapotranspiration, which does not take into account the water level. With less available water in the green roof, the rate of evapotranspiration decreases as the soil/vegetation resistance from the remaining water becomes stronger. A study of the results from Lundstedt & Karlsson (2003) shows a quadratic-like relationship of evapotranspiration to the amount of water in the green roof. This model is based on that relationship.

$$Q_E = K^*(1-h_r)w_a{}^2 \tag{16}$$

In order to calculate the amount of water Q_E translates into, the latent heat of vaporization (λ) is used with equation 17. λ changes very little with even large temperature differences. Nevertheless, assuming that the water temperature on the surface is the same as the surface temperature, a constant value was chosen after examining the mean daily surface temperature on evaporative surfaces for the two months. The mean temperature was about 26° C, which corresponds to a latent heat of vaporization of 2.44 MJ kg^{-1} K^{-1}.

$$E = Q_E / \lambda \tag{17}$$

This formula was validated using laboratory experiments from Lundstedt & Karlsson (2003) in which experiments are made to measure the weight of a small green roof in a laboratory. Rates for evaporation come very close to these values and make this formula a decent approximation.

Now all the necessary inputs for the surface temperature (T_s) equation are known and T_s is calculated using the energy balance equation (Eq. 18), modified from its original appearance.

$$K^* + L\downarrow = \varepsilon\sigma T_s{}^4 + h_c(T_s - T_a) + Q_E + Q_S \tag{18}$$

5.1.8 Drainage materials

Runoff depends on the water holding capacity of the soil substrate and the drainage material. This study uses materials from *Veg Tech* that are suitable as a drainage layer (Table 2). *Nophadrain* consists of a polystyrene mat with small cups that hold water and is offered in two different types. *4+1* is 11 mm thick and is made for slopes between 2-5 degrees and the thicker *5+1* is suitable for flat roofs. *5+1* has twice the water holding capacity of *4+1*. One of the reasons for a thicker drainage layer for flat roofs is minimizing the potential for some rainwater to accumulate in small depressions on the roof, therefore causing a wet substrate which may lead to development of weed. *VT* is made from recycled fiber textiles and its water holding capacity decreases with increasing slope. For 5-10 degree slopes the retention is 8 mm, but for 20-25 degree slopes the retention is 5 mm. The elevation of the area is rather high and exposure to wind may require the use of the drainage material *Hydrofelt*, which can hold 8 mm and is especially suited for windy conditions.

Table 2. Drainage materials

	Nophadrain 4+1	Nophadrain 5+1	VT
Thickness (mm)	11	25	10
Slope °	2-5	<2	>5
Slope in model °	0-5	0	>5
Capacity (mm)	1.6	3.2	5-8

For soil substrate, 10 mm water holding capacity is chosen after a review of Bengtsson (2002), Villarreal *et al*. (2004) and Lundstedt & Karlsson (2003). Green roofs have both a lag (detention) effect and peak reduction (attenuation) effect. The detention effect is not included in the model but runoff will occur only after field capacity has been filled, which in reality may start somewhat sooner (Bengtsson, 2002).

5.2 Extracting roof properties

Field studies were performed on two occasions (25/4 and 9/5) and a total of 247 photos were taken with a digital camera in order to study the area and its buildings. The main purpose was to find the slope of each roof section and the type of roof coating/material used. A roof section is defined as a roof or part of a roof where the material, slope and aspect are the same. Slopes were divided into seven classes of five degree intervals and some tools were used to estimate the slope. Most slopes were extracted by studying the digital photos on a computer screen. The university hospital was of great help due to its tall structure and high elevation since the majority of the area, including all nearby roofs, could be accessed visually from the top 12th floor. Some roof areas were either to steep or to complex to generalize due to time constraints.

5-degree intervals for roof slope seemed to be a reasonable compromise between how exact slopes would be able to be measured and the needed accuracy. Also, the limit for one drainage material and the ability for on-site establishment is at 5 degrees. The middle value of a certain class is used for calculations, i.e. if the roof is classified into group 3 (which has a 5-10 degree angle), the value used for calculations is 7.5. The true area of the roof is calculated using the slope and the horizontal area of roof occupancy (true area = horizontal area / cos(slope)).

High resolution orthophotos of the area from June 2004 with a resolution of 0.5 m were obtained from the city's technical administration. Additional orthophotos from 2000 covering the eastern half the area with a resolution of 0.2 m were provided by the department of Physical Geography and Ecosystems Analysis. These orthophotos were useful for information about the roof properties and especially when dividing roofs into roof sections, as will be described below.

Even if a roof has the appropriate slope and material for green roofs, there are several areas that are unsuitable, such as chimneys, fans or loft windows. A study of the aerial photographs of the area shows that this mostly applies to old and often sloped roofs (Figure 6). Extracting these features in the GIS would be very time consuming and areas are considered small enough to be left out of the model. Even though not the whole area is covered by a green roof, the water that falls on the areas not covered by the green roof is certain to flow into the green roof at some time, and thus contributes to the water storage. Using a potential green area of 100% means that the water storage capacity of the actual green roof is slightly overestimated.

5.3 Creating a GIS

A datasheet containing information on all buildings in Lund as of October 2004 was also obtained from the city's technical administration. The detail of the data is aimed at good representation at a scale of 1:5000, so a small generalization is accepted. When working with the datasheet to divide roofs into sections, all details visible in the orthophotos were represented on the digital map. This implies a high accuracy. Some buildings had areas that did not qualify as roof areas and these were placed in category *other*. These include structures unfit for green roofs such as roof covered with fans, the university hospital helipad and the Allhelgona Church. Generalizations were made on two buildings where roof sections were complex, one of which was the main building of the university hospital. The roof will be treated as a class two but without a specific slope. GIS work was performed in ArcView 3.x and the freeware program fGIS[2].

5.4 Model

One of the purposes of the model was that it should be applicable to any roof areas and that it provides many changeable parameters. Input was provided in tab-delimited text files and the flexibility of the model demanded complex programmable functions, so for this purpose Matlab 7.0.1 was used. Raw input data was edited in Microsoft Excel before text file export. The needed climate input data were measured shortwave radiation (R_{net}), humidity (h_r) and air temperature (T_a). Pressure, wind speed and wind direction were also available, but not used. The program used several functions to complete the different calculations. The order of the main steps performed were:

1. Define parameters and import files
2. Set area variables
3. Import roof data and set green roof suitability
4. Import climate data (R_{net}, h_r, T_a)
5. Import solar position data (ψ, φ_S)

[2] Developed by the University of Wisconsin and Department of Natural Resources division of forestry.

6. Import properties of roof materials *(α, ε)*
7. Set green roofs on/off
8. Calculate solar angle *(θ)*
9. Calculate transmissivity *(τ)*
10. Calculate shortwave radiation ($K\downarrow$, $K\uparrow$, K^*)
11. Calculate water level and evaporation (Q_E)
12. Calculate longwave radiation in ($L\downarrow$)
13. Calculate surface temperature (T_s)
14. Calculate longwave radiation out ($L\uparrow$)
15. Calculate radiation balance (L^*, Q_H, Q_E, Q_S, Q^*)
16. Calculate summaries and averages
17. Output data / graphics

6 Simulations

6.1 Standard roof comparison with sensitivity analysis

A simple comparison was made between a hard roof and a green roof. The most common roof material in the area was a flat bituminous roof, and so this was chosen as the hard roof material (further details about the roofs are presented in the results). The two surfaces were tested for two separate climatic conditions, assessed from two typical midday July values of a cold cloudy day and a warm sunny day (Table 3). To further test the reliability of the evapotranspiration in the model and how it affects the end results, two water levels were tested: 50% (6.6 mm) and 100% (13.2 mm) as well as a green roof without water. This gives a total of eight different scenarios.

Table 3. Climate scenarios for sensitivity analysis.

	R_{net} (W m^{-2})	T_a (C)	h_r	Ψ
Sunny	800	25	50%	40
Cloudy	300	15	75%	40

These scenarios were also used for testing the sensitivity of the chosen variables albedo (α), emissivity (ε), convection coefficient (h_c) and Q_S /Q^* daytime ratio. Given the number of parameters to be tested and the many calculations that are performed in the model, a stochastic Monte Carlo approach was appropriate. The first step in this process is to evaluate or determine the error than can exist in each parameter. Then the model is run many times while randomly choosing a value for each parameter within the error range. Estimated error values (Table 4) for different parameters are based on ranges found in literature, previous research or personal judgment.

Table 4. Parameters with error ranges tested in Monte Carlo simulation.

		Value	Estimated error	Range
albedo α	bituminous	0.15	+/- 0.05	0.1 – 0.2
	green roof	0.25	+/- 0.05	0.2 – 0.3
emissivity ε	bituminous	0.90	+/- 0.025	0.875 – 0.925
	green roof	0.95	+/- 0.025	0.925 – 0.975
convection coefficient h_c		12	+/- 2	10 – 14
Q_S/Q^* ratio		-0.15	+/- 0.05	-0.1 – -0.2

The most interesting results from the sensitivity analysis are those for Q^*, Q_H and Q_E. An interesting value to look at under natural conditions would be Q_S, but since this model uses the storage heat as an input rather than an output, it is not valid as a comparison value. Some of the parameters in Table 4 have direct effects on some values, such as h_c on Q_H. Therefore sensitivity is measured each parameter at a time as well to complement the Monte Carlo simulation.

Runoff reduction values on a monthly basis were also calculated on the simple roof surface. This makes an easy comparison with other studies since these often focus on green roofs and not total roof areas. Runoff was also calculated using different values for field capacity to study possible effects of the use of some intensive green roofs, or to see the sensitivity of the chosen field capacity value.

6.2 Design rains

Runoff was studied for design rains without consideration for radiation balance. The main principle of design rains is that the more intense the rain, the less frequent it is. Design rains function as mathematical approximations of rains with various intensities, lengths and return periods. Niemczynowicz (1984) studied rain dynamics for Lund and created commonly used intensity-duration-frequency (i-d-f) curves using 12 rain gauges over a period of three years. They are represented by equation 19.

$$I = \frac{a}{T+b} + c \qquad (19)$$

Constants *a*, *b* and *c* are site specific for Lund and exist for different area sizes. *I* is the rain intensity (mm/min) and *T* is the duration in minutes. Values for an area of 2.1 km^2 are chosen, which most closely matches the size of the study area. Green roofs are expected to delay the peak runoff volume and also the total runoff volume. Two different results are presented for design rains. First, only the area of the roofs is studied. Then the total study area is modeled with a green space factor for the whole area.

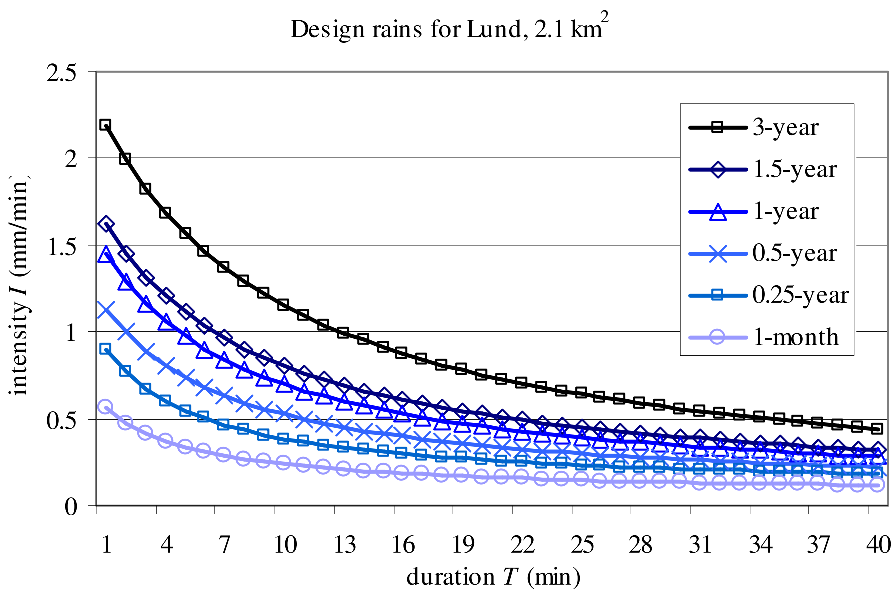

Figure 8. Design rains for Lund. Intensity as a function of duration, where curves show the mean intensity for a rain of a particular duration.

6.3 Monthly simulation

Two months were simulated; July and August 2004. These months were chosen for their high temperatures and chances of intense rain periods with flooding potential. In addition, the two months together display one month with normal conditions and one with excessive rain. July was a rainy month in Lund with 128 mm of rain (normal[3] 70 mm) whereas August had a close to normal 73 mm (normal 65 mm). The daily precipitation data is dispersed evenly over a 24 hour period since the time, duration, length and intensity of each rain event is not known. The precipitation data for each day is originally measured at 7 am and is thus an equal value is given each timestep in the model for the 24 preceding hours. Water levels at the start of each simulation were set using results from a 10-day simulation before the July period and using the July end water levels for the August simulation.

[3] 1961-1990 average

7 Results

7.1 Roof data and green roof potential

The potential for green roofs were 85.17% of municipal roof areas, which equals 13.66% of the whole study area. One reason this area was chosen as a study area was its high share of municipal buildings, as shown in Table 5. One aim of green roofs and ecological construction in general is to increase permeable areas. Green roofs do not qualify as permeable areas but nevertheless share some of the characteristics of permeable areas, such as retaining water and cooling the surface through latent heat release. An estimation of the share of green areas in the study area was made and it suggests that the use of green roofs would increase green areas from 41.8% to 55.4%, an increase of roughly 1/3, or 33%.

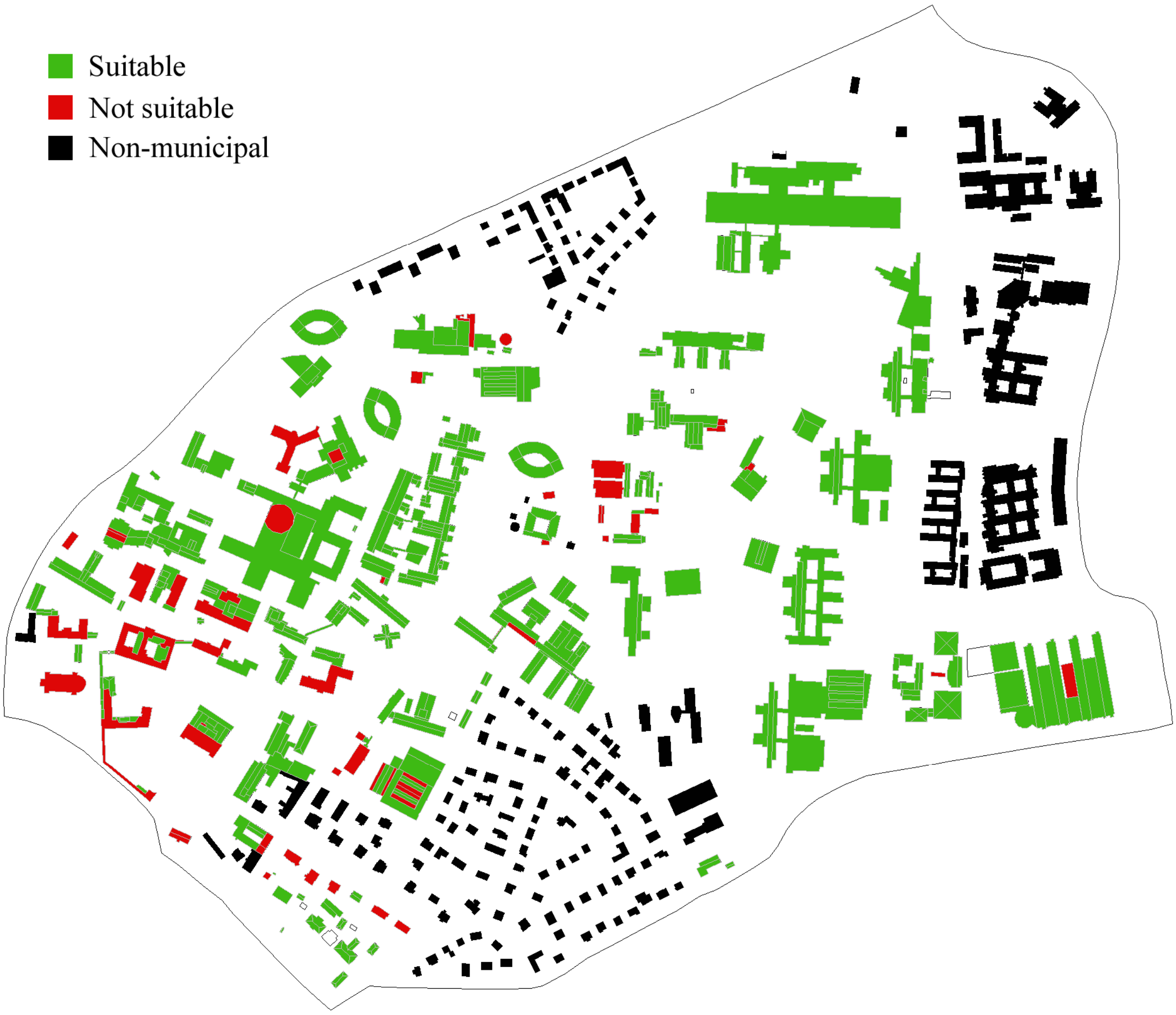

Figure 9. Buildings divided into roof sections. Areas suitable for green roofs are shown in green and unsuitable roofs are in red. Black buildings are non-municipal.

Table 5. Area surface distribution. A few green roofs already exist in the area.

Surface				Area (m²)	Share (%)
Permeable				587 851	41.67
Impervious	Other			525 078	37.22
	Buildings	Non-municipal		71 527	5.07
		Municipal	Unsuitable	32 352	2.29
			Suitable	192 711	13.66
			Green roofs	1 211	0.09
Total				**1 410 729**	**100.00**

As seen in Table 6, roof surface consists dominantly of a bituminous material (62.9%). This is a good roof surface material to construct green roofs on and it represents 72.67% of all suitable roof surfaces. Metal roofing, especially grey, is the second most common material (11.2%) and many of the older buildings with higher roof slopes have tile roofing. The roof material category *other* consists of various surfaces without a typical roof surface, such as a chimney. This category, along with glass, are considered unsuitable for green roofs. Flat roofs are most common with an area cover of 42%, whereas slopes between >0 and 5 degrees account for 25%. This large share of flat and low sloping roofs allows for on-site planting of sedum cuttings. This is a less expensive alternative to prefabricated vegetation, which is required for slopes above five degrees. The remaining roof slope classes are each under 10%. Slopes above 25 degrees, which is considered a limit for this study, cover 11.5% of the roof area. This class includes the various untypical roof surfaces mentioned above.

Table 6. Slope and material distribution (m²). Shaded cells indicate slopes and materials considered for green roof application.

		Slope									
		0	**0-5**	**5-10**	**10-15**	**15-20**	**20-25**	**25-30**	**other**	**Total**	**%**
Material	bituminous	81316	37670	5854	11894	2612	704		1503	**141552**	**62.9**
	concrete	5551								**5551**	**2.5**
	metal black		288	150	300			600		**1338**	**0.6**
	metal green		407			4413				**4820**	**2.1**
	metal grey	3513	12432	1036	6820	163	947	149	101	**25162**	**11.2**
	metal white	376	5259	1048	797		1614		287	**9382**	**4.2**
	tile dark						214	118	10125	**10457**	**4.6**
	tile light					2192	5067	2571	7634	**17464**	**7.8**
	glass						2301		348	**2650**	**1.2**
	green roof	771	76	364						**1211**	**0.5**
	other	2942							2461	**5403**	**2.4**
	Total	**94470**	**56132**	**8451**	**19811**	**9381**	**10847**	**3438**	**22460**		
	%	**42.0**	**24.9**	**3.8**	**8.8**	**4.2**	**4.8**	**1.5**	**10.0**		

7.2 Standard roof comparison with sensitivity analysis

7.2.1 Energy balance

Results from the flat roof comparison are seen in Figure 10. Stochastic Monte Carlo simulations are presented with standard deviations. In sunny conditions Q^* is highest for a green roof with water available for evapotranspiration. This Q^* is balanced by a small Q_H and a high Q_E. Without available water, Q^* decreases and Q_H is much larger. A hard bitumen roof shows even higher values of Q_H. Standard deviations are highest for sensible heat.

In cloudy conditions there is much less Q^*, but it is highest for the hard roof. On a green roof with evapotranspiration Q_H is higher than Q_E, in contrast to sunny conditions. Q_H is increased for a green roof without water and even more for the hard roof. The standard deviation is highest in Q_H and smallest for Q_E. Even without water a green roof has lower values of Q^* and Q_H than a hard bitumen roof in both cloudy and sunny conditions.

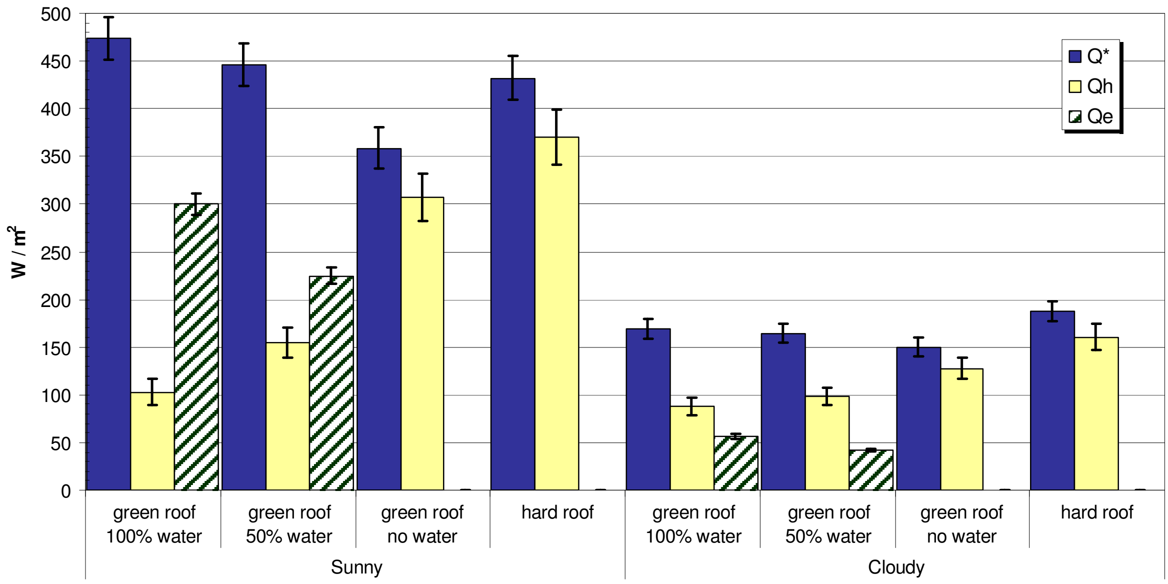

Figure 10. Bitumen vs. green roof comparison using a Monte Carlo simulation. Average values are shown with error bars indicating standard deviation. Q_H and Q_E are shown with positive values instead of negative.

The results from the Monte Carlo simulation can be compared with the results from the standard simulation with parameters unchanged. Values indicate small differences, with the highest values attributed to Q_H (Table 7). All anomaly values are within 0.6%, which suggests that any inaccurate parameter values will only slightly change the results more in one direction than the other.

Table 7. Difference between standard simulation and Monte Carlo average (%).

		Q^*	Q_H	Q_E
Sunny	green roof 100% water	0.09	0.02	0.06
	green roof 50% water	0.17	-0.29	0.08
	green roof no water	0.20	-0.35	-
	hard roof	0.32	-0.44	-
Cloudy	green roof 100% water	0.05	-0.20	0.00
	green roof 50% water	0.18	-0.45	0.04
	green roof no water	0.36	-0.49	-
	hard roof	0.29	-0.60	-

A sensitivity analysis changing only one of the parameters (Table 4) at a time was also performed. This showed small changes in most cases. Largest differences were found for Q_H, which changed up to 10% for ±0.05 albedo changes and up to 18% for ±0.05 Q_S/Q^* changes. Also, Q_H was most sensitive when there was evapotranspiration. More detailed values are presented in appendix A.

7.2.2 Monthly runoff

An estimate of the effect of a change from a hard roof to a green roof is given in Table 8. The decrease in runoff for July and August for the flat surface was 22.7% and 59.6%, respectively. The green roof water level was at its highest at the start of July (13.2 mm), then very low at the beginning of August and again at field capacity at the end of the month. The runoff reduction for the two month period was 36%.

Table 8. Runoff (*R*) reduction for standard roof comparison. Values in mm = liters per square meter.

	P	*R*	reduction	reduction (%)	*E*	storage change
July	128.16	99.42	28.73	22.42	40.52	-11.79
August	73.22	29.47	43.75	59.75	31.96	11.79
Total	201.37	128.89	72.48	35.99	72.48	0.00

The effect of an increase or decrease in substrate field capacity was very small. 15% changes in water holding capacity of the green roof affected evapotranspiration in July with roughly 4% and runoff in August with less than 6%. Differences are to some degree caused by water level changes at the end of July. However, concatenating the two months and thus eliminating water level changes shows discrepancy values of between 1.2% and 2.8%, with *E* slightly more affected than *R*.

Table 9. Changes in runoff (*R*) and evapotranspiration (*E*) for ±15% changes in total field capacity (substrate + drainage layer).

	8 mm (-15%)		12 mm (+15%)	
	R	***E***	***R***	***E***
July	0.3	-4.3	-0.2	3.4
August	5.7	-1.0	-4.4	0.4
Total	1.6	-2.8	-1.2	2.1

7.3 Design rains

7.3.1 Peak delay

Results show a delayed peak in runoff and lowered runoff volume, giving the potential of an attenuation effect as well. Green roofs with no initial water were only saturated by the 20-, 30- and 40-minute rain of the three year design. Therefore only the results for initial water levels of 50% are presented (Table 10). None of the one-month rains saturated the green roofs. With the assumption that other permeable areas do not saturate, the peak runoff delay will be the same for the whole area as it is for the roofs.

Table 10. Peak runoff delay (min) for study area with the use of green roofs for different design rains. Initial water level in green roofs are 50% of capacity. Missing values indicate green roofs that did not saturate.

	Duration (min)					
	5	**10**	**15**	**20**	**30**	**40**
3-year	4	5	7	9	12	15
1.5-year	-	8	10	13	17	21
1-year	-	9	12	15	19	24
0.5-year	-	-	-	19	25	31
0.25-year	-	-	-	-	-	37
1-month	-	-	-	-	-	-

7.3.2 Volume reduction

The storage capacity of rainwater in all green roofs equals 2,625 m^3. As discussed previously, an initial dry state will only saturate three design rains, leading to volume reductions being equal to the rain volume in remaining designs. Volume reduction in Figure 11a is calculated using a 50% of field capacity initial water level, which for the monthly climate simulations described later is a common value. The resulting values are either the same as remaining free storage (1,313 m^3) or the total rain amount. Figure 11b shows a maximum runoff reduction of 24%, which corresponds to the share of impervious area turned into green roofs. The less common and heavy 3-year rains fill the green roofs to storage capacity but reduction in this scenario is still 21% for the 5-minute rain and 9% for the 40-minute rain.

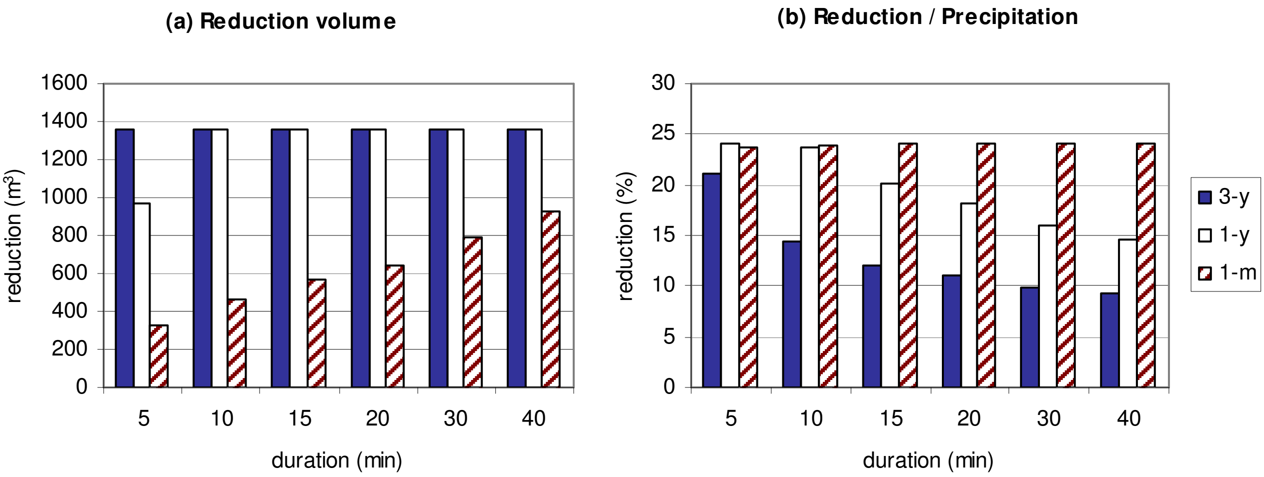

Figure 11. Volume reduction in thousand m^3 (a) and share of total precipitation (b) for total area with the use of green roofs. Initial water levels are 50%. Design scenarios for 3-year, 1-year and 1-month rains are presented.

7.4 Monthly simulation

7.4.1 Monthly radiation

The radiation balance is mainly affected by the incoming solar radiation and the water availability. One day can be very different from the next and typical variations can be seen in Figure 12, which shows ten days in August. Q_H is significantly greater for simulations without green roofs and reaches over 350 W m^{-2} on clear days (days 5-10). Days one and two exhibit partly cloudiness with some noticeable Q_H peaks at the same levels as a clear day. The third day represents an overcast day and all radiation levels are very low. Without green roofs Q^* peaks at about 400 W m^{-2} on the clearest days (5-10). However, with the use of green roofs Q^* is higher on day 5 but decreases over time as water levels decrease. The reduction in evapotranspiration, caused by less available water, is somewhat matched by an increase in Q_H, but Q^* decreases. Longwave radiation seems to be lower for green roofs when these have water available for E. Complete monthly simulation results are shown in appendix B.

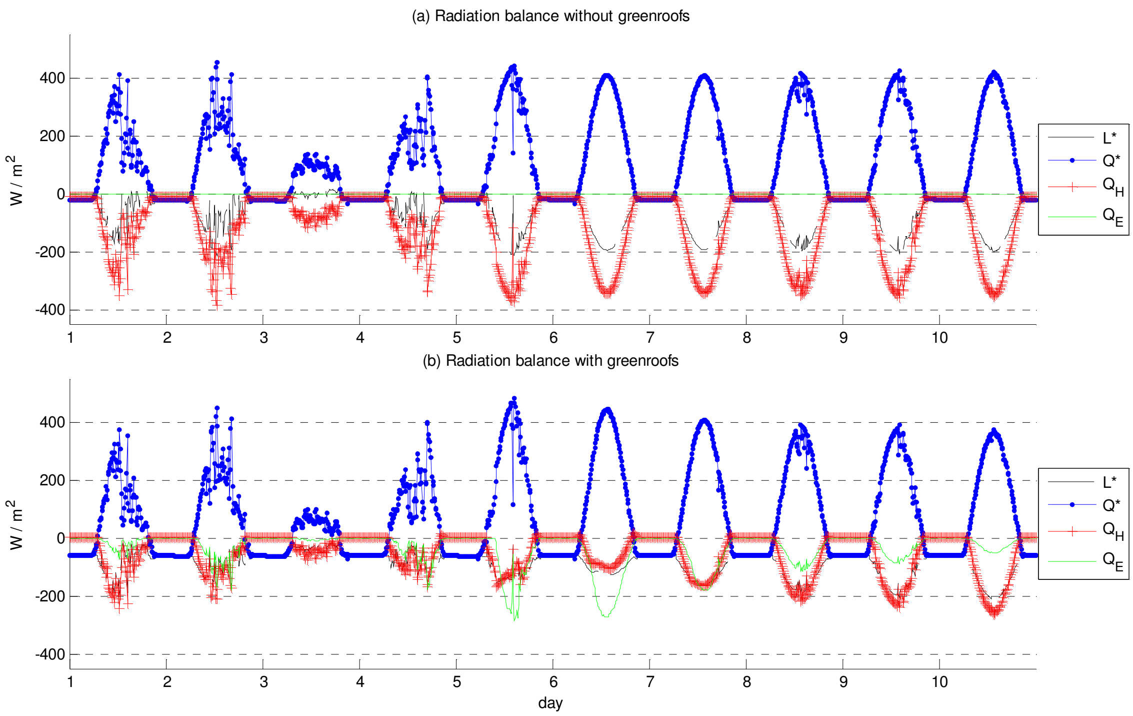

Figure 12. Excerpt of monthly simulation for 10 days in August without (a) and with (b) green roofs.

7.4.2 Surface temperature

Green roofs reduce surface temperature during the day, as seen in Figure 13. Despite the lower course of the sun, temperatures were higher for August than July due to more sunny days. Surface temperatures are lowest just before sunrise and peak between noon and 2 pm.

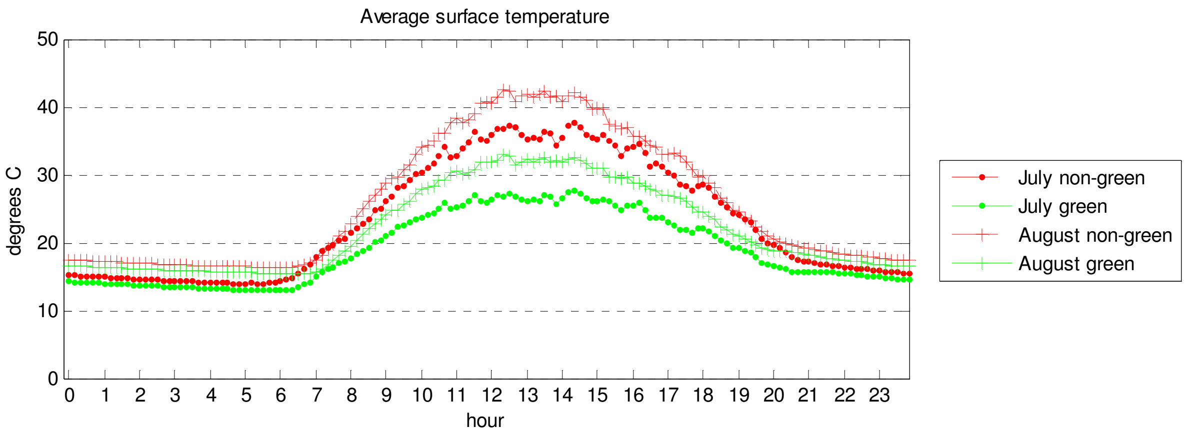

Figure 13. Monthly average surface temperatures.

Daytime (1100-1500) average surface temperatures are shown in Table 11. Green roofs reduce daytime T_s by 9.3 degrees in July and 9.0 degrees in August.

Table 11. Average daytime surface temperatures.

	non-green	green	change
July	35.7	26.4	-9.3
August	40.7	31.7	-9.0

7.4.3 Average daily radiation balance

The impact of green roofs over the course of a month is most easily shown using an average of the daily radiation, as seen in Figure 14 and Figure 15. July and August are studied before (a) and after (b) the application of green roofs. Q^* is higher in August than July, which corresponds well with the higher rainfall in July. Q_E seems to be slightly higher in July, although Q^* was lower. Higher water levels increases Q_E, which can counter effect the decrease in $K\downarrow$. One of the most visible differences with and without green roofs is net radiation during night. Green roofs have a higher emissivity than hard roofs and especially uncoated metal roofs, causing a higher $L\uparrow$ than the simulated $L\downarrow$. The effect is diurnal, but is most visible when there is no shortwave radiation, i.e. at night. This results in a significant decrease in nighttime net radiation with the use of green roofs. Another feature is the decrease in Q_H, a consequence of lower surfaces temperatures for green roofs.

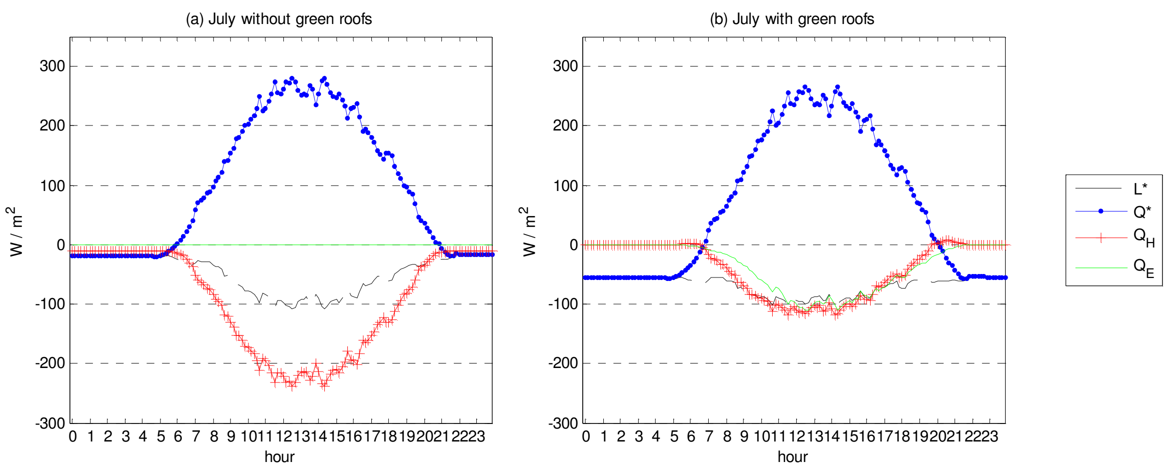

Figure 14. July simulation without (a) and with (b) green roofs.

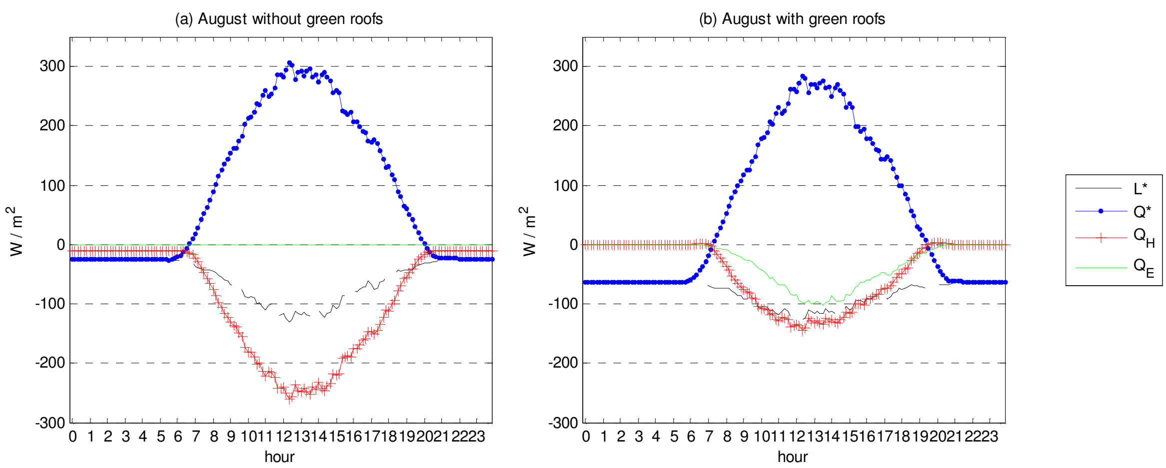

Figure 15. August simulation without (a) and with (b) green roofs.

Green roof impact is shown directly in Figure 16. Both Q_H and Q_E have higher differences in July than in August, but overall the differences between the two months is small. The shorter day length of August is visible by the more narrow width in the figure. The decrease in longwave radiation occurs almost throughout the whole day, leading to a decrease in net radiation.

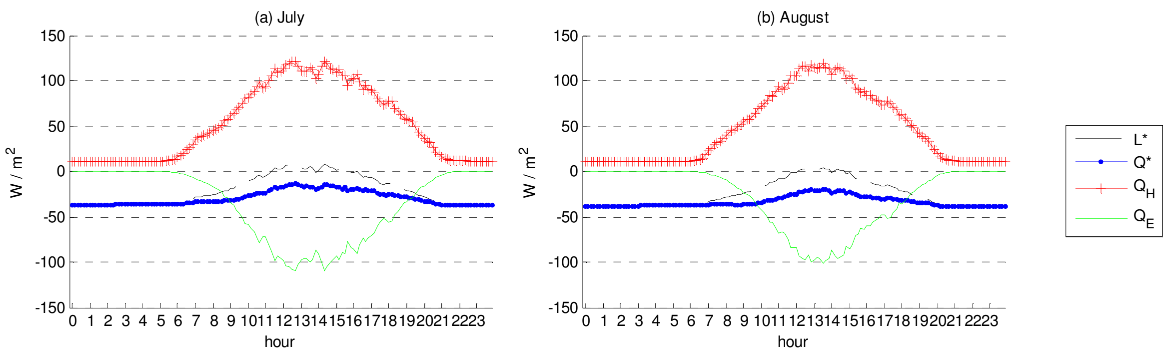

Figure 16. Green roof impact on radiation balance for July (a) and August (b). Values shown are changes brought from green roofs.

7.4.4 Average daytime and total radiation

Daytime averages are calculated using values between 11 am and 15 pm, in reference to Christen & Vogt (2004). July and August show a decrease in Q_H that is close to the same as the increase in Q_E (Table 12). July has a slight increase in Q^* with green roofs, whereas August has a small decrease. The Bowen ratio is lowest for July with a value of 1.12, meaning almost equal amounts of Q_H and Q_E.

Table 12. Daytime (1100-1500) average values for July and August with and without green roofs.

		Q^*	Q_H	Q_E	*Bowen*
July	non-green	258.4	-219.2	-0.6	
	green	240.8	-108.1	-96.9	1.12
August	non-green	280.0	-237.7	-0.6	
	green	256.6	-129.8	-88.6	1.47

Monthly totals are presented in Table 13. Q^* decreases with green roofs largely due to lower nighttime values and more for August than July. Q_H is halved with green roofs and Q_H and Q_E are slightly more affected in July than in August.

Table 13. Monthly average daily values of total radiation (MJ m^{-2}) for July and August with and without green roofs.

	Q^*	Q_H	Q_E
July non-green	8.36	-7.98	-0.02
July green	5.80	-3.48	-3.10
Change	**-2.56**	**4.50**	**-3.08**
August non-green	7.81	-7.85	-0.02
August green	4.90	-3.87	-2.43
Change	**-2.91**	**3.98**	**-2.42**

7.4.5 Runoff

A comparison between the current roofs and the use of green roofs shows a significant decrease in runoff for August, a month with close to average rainfall. The decrease for the roof areas is 58.2% or roughly 42 mm and for the total area 14.1% (6 mm), using the estimated amount of permeable areas (Table 14). The decrease in July is less significant (21.8% or 27.5 mm vs. 5.3 or 4%) since higher amounts of rain keep the water levels close to storage capacity during most of the month. Figure 17 shows accumulative precipitation and runoff.

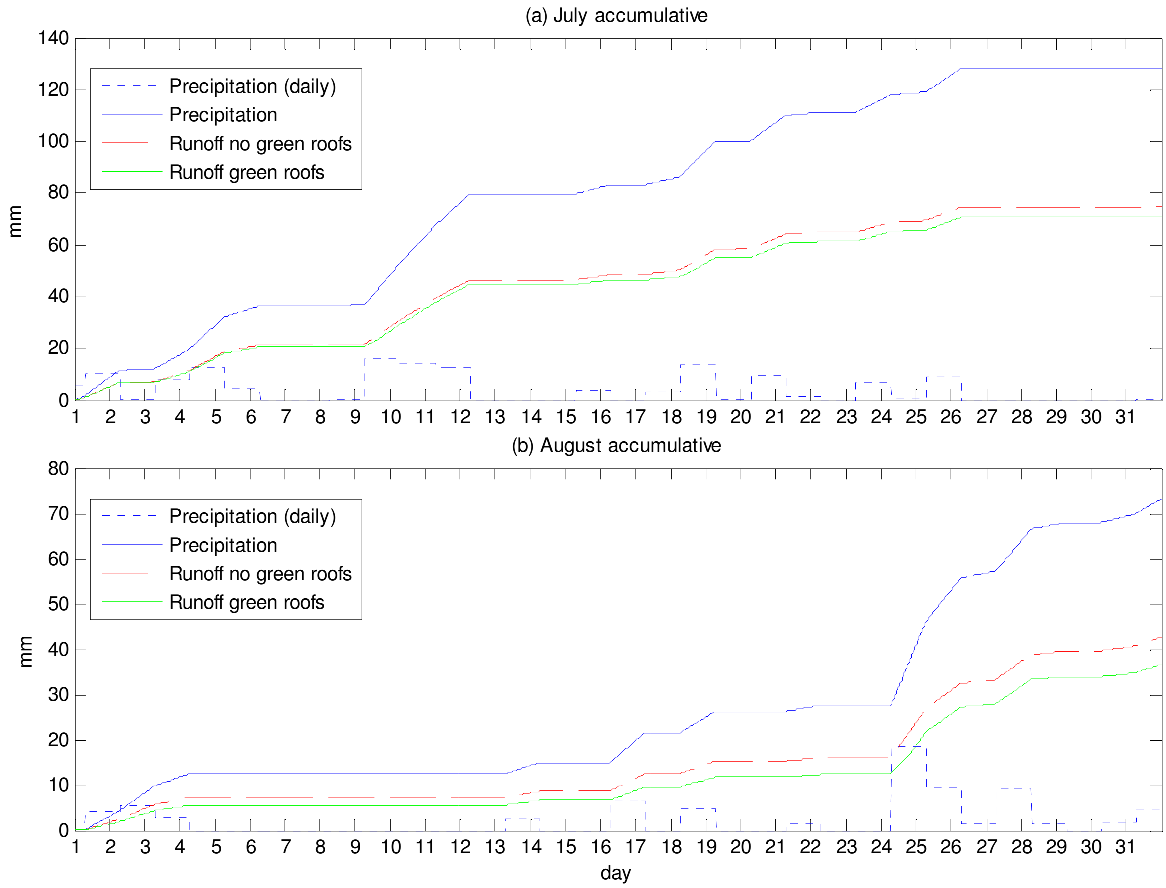

Figure 17. Accumulated precipitation and runoff with and without the use of green roofs for study area under July (a) and August (b). Note the different scaling on the y-axis.

Table 14. Water balance (mm) for July and August with and without application of green roofs.

	P	***R***				***E***		**Storage change**	
		non-green	**green**	**change**	**change (%)**	**non-green**	**green**	**non-green**	**green**
July (roofs)	128.16	126.47	98.94	-27.53	-21.8	1.76	40.64	-0.07	-11.42
July (area)	128.16	74.71	70.77	-3.94	-5.3	-	-	-	-
August (roofs)	73.13	72.09	30.15	-41.94	-58.2	0.97	31.54	0.07	11.44
August (area)	73.13	42.66	36.66	-6.00	-14.1	-	-	-	-

7.5 Cost analysis

Most buildings were larger than 5,000 m^2 and thus cost was calculated using the price for areas of that size and are presented in Table 15. These costs should be weighed against the direct and indirect financial benefits of green roofs, as well as aesthetic value. Prices are calculated for materials from and installation by *Veg Tech*.

Table 15. Cost for establishment of green roofs on all suitable areas (excluding tax).

	Slope			Total	SEK m^{-2}
	0	**0-5**	**5-25**		
Area (m^2)	90 756	56 110	47 535	194 401	
Prefabricated cost / m^2	469	441	409		
Extra costs / m^2			45		
Total cost	**42 564 653**	**24 744 384**	**21 580 945**	**88 889 982**	**457**
On-site cost / m^2	383	357	-		
Extra costs / m^2			45		
Total cost	**34 759 621**	**20 031 168**	**21 580 945**	**76 371 734**	**393**

The calculated total cost is about 76 million SEK (excluding tax) using on-site establishment when possible and roughly 89 million SEK when using only prefabricated mats. Cost per square meter is at best less than 400 SEK.

8 Discussion

8.1 Study area and roofs

Municipal buildings occupy a very large share of the study area surface, with 85% of these suitable for green roofs according to the criteria in this study. The true area is expected to be slightly lower since some areas of the roof are occupied by chimneys and ventilation pipes. Flat roofs and low sloping roofs offer the ability for constructing green roofs on-site, thus keeping down cost. The area is situated rather high, which has to be taken into consideration for some sloped roofs exposed to high winds. Bituminous roofs account for about 73% of all suitable roofs, which is good because they need little preparation. The large University Hospital and large buildings of LTH are very suitable for green roofs since they offer large areas with little slope and few obstructions. Tall buildings such as the hospital would probably need a large crane for transporting material to the roof. In reality there may be areas of a roof that are unsuitable for green roofs, such as areas in constant shade or in a rain shadow, but an evaluation of the site found very few such areas. A potential increase in green areas of 1/3 is very good considering no alteration of ground surfaces.

8.2 Sensitivity analysis

Standard deviations for different Monte Carlo simulations were found to be low and in most cases are not significant enough to question differences between simulations. Changes in value for Q_H are highest when there is evapotranspiration. This can be explained by evapotranspiration not being connected to the other variables – it is calculated using only the net shortwave radiation. A change in albedo seems to have most effect overall. This is not surprising since it changes K^*, which in turn affects the entire radiation balance. Changing the convection coefficient h_c does not have that much effect on Q_H since T_s changes with different h_c values and minimizes the potential changes in Q_H.

8.3 Runoff

Design rains with no initial water on green roofs only saturated for the precipitation intense 3-year design rains, which shows that green roofs can be very good at reducing runoff under dry initial conditions. However, even with 50% initial water levels the runoff reduction on the heaviest rains was about 10-20%.

Rain events are represented on a daily resolution, which is often the most detailed data available for monthly climate simulations unless measurements are carried out for the purpose of a specific study. A resolution of precipitation data down to hours or minutes would likely have a very small impact on the energy balance equation. The benefit of detailed precipitation data would be to see more clear effects on runoff detention, attenuation and peak reduction. However, these effects can easily be simulated with the design rains without consideration for the energy balance. Runoff detention is a documented effect of green roofs with suggested values of 20 minutes (Bengtsson, 2002) for water to flow through the substrate. If this were included in the simulation of the design rains, the expected effect would be an even more delayed and reduced peak flow. Retention is decided by almost all factors; the saturation of the green roof, the composition of substrate and drainage layer and the length and slope of the roof.

Some limited rainwater can accumulate on flat roofs, but no research was found to indicate the amount of storage on flat roofs, leading to the assumption that such storage is rather small and perhaps not enough to have an effect on the model. Rain showers can often be directly followed by evapotranspiration and this is included in the model since evapotranspiration is only dependent on K^* and humidity. The monthly simulations on all roofs, which includes many non-green roofs, overall shows very similar results to the standard simulation on one flat green roof. This could be explained by the higher drainage layer storage in sloped roofs compensating for lower storage in flat roof drainage layers.

July has more runoff due to a higher rainfall amount. However, the high rainfall also amounts to less effect with green roofs. The saturation of the green roof occurs more often during July and thus runoff will be higher. The highest green roof effect would be achieved for weather with rain events every second or third day, saturating the green roof and leaving time for evapotranspiration until the next rain event. Another scenario is a dominance of light rains that are very effectively retained by green roofs (VanWoert, 2005).

Combined sewers are only found in a small part of the area. The potential decrease in runoff will have most economic benefits from this small area. On the other hand, separate sewers should still be encouraged even if green roofs are combined with ponds to retain and detain water since areas such as roads and parking lots remain as stormwater sources.

The simple method of evapotranspiration correlates well with Lundstedt & Karlsson (2003), but measurements from that study occurred under constrained climatic conditions, albeit different green roof conditions. Although there are many studies on latent heat release from grasses, crops and forests, the specific buildup of a green roof calls for research focused specifically on green roofs. Therefore, a more elaborate study would be preferred in order to accurately estimate the evapotranspiration rate from green roofs. Any overestimation of the evapotranspiration would lead to decreased simulated runoff and cooling benefits from green roofs. Contrary to VanWoert (2005), field capacity has very little effect on evapotranspiration in these simulations.

8.4 Energy balance

This model only takes into account storage heat through the roof and not other important fluxes like heat storage in walls, roads, etc. These other fluxes also affect the city climate and thus results of roof surface simulations are difficult to translate into urban climate changes. Winds move air across roof surfaces and into urban canyons, so some change in urban canyon temperatures would be expected. In addition, it has previously been explained that radiation is trapped in urban canyons, and an urban canyon with higher air temperatures than the surrounding air will cause that air to rise upward. At the same time, cooler air above green roofs will tend to flow into the urban canyon to replace the rising air. Urban heat islands lead to lower wind speeds in the city and thus a higher possibility for polluted air to remain close to the urban surface (Akbari *et al.*, 2001). If green roofs lower the urban temperature, they may also increase the air quality in the city by increasing the convection of air.

This model only needs a measure of R_{net} or simulated $K\downarrow$ and humidity to simulate Q_E. To further test the accuracy of calculated Q_E comparisons with other models would be appropriate. The convection coefficient works well with the model and does not have a significant effect on sensible heat. However, the model might be more accurate if the vertical wind component is included. Daytime simulations are most reliable since nighttime cloudiness is not known and the average daytime cloudiness is used to calculate nighttime $L\downarrow$.

Surface temperatures are significantly lowered with the use of green roofs and this reduction is what decreases both L^* and Q_H, the latter of which causes a decrease in ambient temperature. Even without changing low emissivity metal roofs to high emissivity green roofs, surface temperature is lowered by the use of evapotranspiration. Another benefit from T_s reduction is reduced Q_S, thereby improving insulation from high summer temperatures. If this potential change in Q_S would have been simulated by the model, results may have shown stronger positive effects from green roofs. It is known, however, that reducing Q_H and T_s act to mitigate the urban heat island effect.

Variations in the radiation balance are high, which is why monthly averages are most suitable for comparisons. Q_H is very high for a non-green roof scenario or when there is no water available in the green roofs. The decrease in E with lower water levels helps to keep some water available in the green roofs even several days after a rain event.

Compared to urban and rural radiation values from Christen & Vogt (2004), the daytime net radiation in this model is overall lower and would be expected to be higher. Sensible heat values are about the same whereas latent heat is less than half of Christen & Vogt rural values and about the same as an urban residential area value. By comparing with the measured values in that study, Q_E results from solely green roof surfaces in this model seem to be underestimated.

Typical Bowen ratios in urban areas are 2-5 and in rural areas less than 1 (Christen & Vogt, 2004). Simulations in this model almost achieve this rural area value in July and are a good indication of how green efforts in the city can reach a radiation balance found in rural areas. If evapotranspiration is underestimated, the result would be an even lower Bowen ratio. However, the values achieved in the model only represent the homogenous roof area and not a larger urban area with different surfaces and urban canyons.

8.5 Other issues

If green roofs were to be established on this area on a large scale some recommendations can be made, such as those seen in Figure 5. The first is to vary the type of green roof or vegetation for increased biodiversity. Accessible roofs on any University Hospital building should be considered for intensive green roofs if weight requirements on the roof are met. Another approach is to collect the runoff water from all roofs and use this for watering, washing, etc. Many impervious areas such as parking lots can have asphalt replaced with materials that can carry heavy loads while at the same time allowing water to percolate into the ground. Water from other impervious surfaces can be channeled into ponds where it is allowed to evaporate.

8.6 Improving and applying model to other areas

As discussed earlier, some modifications can be made to the model in order to receive more reliable results:

- Sensible heat based on vertical wind component
- Storage heat based on surface temperature and roof properties
- Evapotranspiration results validated using other models
- Runoff detention from green roofs

Using the model on other areas should be easy. Digital maps of buildings exist for all cities in Sweden and most European countries. Some research may be needed to find properties of roof materials that are not used in this study. Climate data that includes radiation is measured continuously in most large cities and even if no appropriate data is available, measurements of a few months are easily made. Including urban canyons is considerably more complicated and should not be attempted for a simple model. Matlab programming was done with the intent to accept any roof or climate data and this was largely achieved, even though a user friendly interface does not exist.

The share of municipal buildings in the study area of this project is very high and a similar study on municipal buildings of another area would probably show less impact of green roofs on the whole area.

8.7 Benefits for Lund

Stormwater management would benefit from using green roofs in the study area since it acts at the source, roofs are considered free space and because dense parts of the area may not allow space for large ponds and channels. The main building of the University Hospital is an especially good candidate since it has large roof surfaces with low slopes that are visible from high floors. In addition to stormwater management, the study by Velasquez (www.greenroofs.com) suggests that green roofs may reduce hazardous birds around the helipad, thereby increasing safety. Aesthetics would be an important factor for the University Hospital area where patients may recover faster in a greener environment.

Many environmental goals in the overview plan would be addressed by the use of green roofs but initial cost is the main barrier to constructing green roofs, which is why they are mostly applied to new buildings. Financial incentives or other greening policies that can lessen the initial barrier is desired. The University, University Hospital and the people who work and study in the area would all benefit from any addition of green roofs to the area.

9 Conclusion

The purpose of this project was outlined in the introduction and all three goals were achieved:

1. A model was successfully created that simulated hydrological and radiative impacts of green roofs on existing buildings.
2. The model was applied to municipal buildings in a sub area of Lund and results showed a positive impact from green roofs.
3. Potential benefits from green roofs and the reliability and flexibility of the model have been discussed.

The clearest results are shown in the potential effects in runoff dynamics and volume. These are also the effects that the city can benefit from the most economically. The building owners themselves benefit from the reduced cost of heating and cooling in the buildings. The people in the area benefit from aesthetics, appearance, less glare, noise and pollution and a more biologically diverse city. The local municipality with its long term plans and goals is ideal for green roof initiatives for two reasons: it may have the ability to look at long term cost and not the initial cost of green roofs and because the municipality, along with the local community, benefit from them the most.

References

Akbari H., Pomerantz M., Taha H. 2001. Cool surfaces and shade trees to reduce energy use and improve air quality in urban areas. *Solar energy* 70: 295-310

Bengtsson L. 2002. Avrinning från gröna tak. (Runoff from green roofs). *Vatten* 58: 245-250.

Berndtsson J.C., Emilsson T., Bengtsson L. 2005. The influence of extensive vegetated roofs on runoff water quality. Submitted.

Bretz S., Akbari H. & Rosenfeld A. 1998. Practical issues for using solar-reflective materials to mitigate urban heat islands. *Atmospheric Environment* 32: 95-101.

Campbell G.S. & Norman J.M. 1998. *An Introduction to Environmental Biophysics*. 2nd Ed. Springer-Verlag New York, Inc. 286 pp.

Christen A. & Vogt R. 2004. Energy and radiation balance of a central European city. *International Journal of Climatology* 24: 1395-1421.

Emilsson T. & Rolf K. 2005. Comparison of establishment methods for extensive green roofs in southern Sweden. *Urban Forestry & Urban Greening* 3: 103-111.

Grezova I. 1997. Inventory of systems for local management of stormwater with an emphasis on "green roofs". Master thesis. Lund University.

Haughton G. & Hunter C. 1994. *Sustainable Cities*. Jessica Kingsley Publishers Ltd.

IPCC. 2001. *Climate Change 2001: Impacts, Adaptation and Vulnerability. Contribution of Working Group II to the Third Assessment Report of the Intergovernmental Panel on Climate Change (IPCC).* James J. McCarthy, Osvaldo F. Canziani, Neil A. Leary, David J. Dokken and Kasey S. White (Eds.). Cambridge University Press: 1000 pp.

Koehler M., Schmidt M., Grimme FW., Laar M. & Gusmao F. 2001. *Urban Water Retention by Greened Roofs in Temperate and Tropical Climate*. 38th IFLA World Congress, International Federation of Landscape Architects, Singapore 2001.

Levinson R., Akbari H., Konopacki S. & Bretz S. 2005. Inclusion of cool roofs in nonresidential Title 24 prescriptive requirements. *Energy Policy* 33: 151-170.

Lindegren D. 2002. *God bebyggd miljö – rapport över miljötillståndet i Lunds kommun. Underlagsrapport för Lunds Agenda 21*. Lunds kommun tryckericentral. 47 pp.

Lundstedt J. & Karlsson P. 2003. Ett grönt taks förmåga att påverka värmetransmission genom en takkonstruktion. Chalmers Tekniska Högskola. 40 pp.

Miljöstrategiska enheten. 2002. *Utvärdering av hur Lunds kommun har levt upp till miljörelaterade ställningstaganden I översiktsplanen från 1998.* Lunds kommun.

Monteith J.L. & Unsworth M.H. 1990. *Principles of Environmental Physics*. 2ed. Routledge, Chapman and Hall, Inc.

Niachou A., Popakonstantinou K., Santamouris M., Tsangrassoulis A. & Mihalakakou G. 2001. Analysis of the green roof thermal properties and investigation of its energy performance. *Energy and Buildings* 33: 719-729.

Offerle B., Grimmond C.S.B. & Fortuniak K. 2005. Heat storage and anthropogenic heat flux in relation to the energy balance of a central European city centre. *International Journal of Climatology* 25: 1405-1419.

Oke T.R. 1987. *Boundary Layer Climates*. 2nd Ed, Cambrige University Press.

Parker D.S., McIlvaine J.E.R, Barkaszi S.F, Beal D.J. & Anello M.T. 2000. Laboratory Testing of the Reflectance Properties of Roofing Material. FSEC-CR670-00. *Florida Solar Energy Center*.

Prado R.T. & Ferreira F. 2005. Measurement of albedo and analysis of its influence the surface temperature of building roof materials. *Energy and Buildings* 37: 295-300.

Sailor D.J. & Fan H. 2002. Modeling the diurnal variability of effective albedo for cities. *Atmospheric Environment* 36: 713-725.

Stadsarkitektkontoret. 1998. *Fördjupning av översiktsplanen för Lund – Universitets-, sjukhus och forskningsområdet.*

Stahre P. 2004. *En långsiktigt hållbar dagvattenhantering*. Svenskt Vatten. 81 pp.

Taha H. 1997. Urban climates and heat islands: albedo, evapotranspiration, and anthropogenic heat. *Energy and Buildings* 25: 99-103.

Ulrich R.S. 2000. *Evidence Based Environmental Design for Improving Medical Outcomes.* Conference proceeding from event at McGill University Health Centre, Montreal.

VanWoert N.D., Rowe B.D., Andresen J.A., Rugh C.L., Fernandez T.R. & Xiao L. 2005. Green Roof Stormwater Retention: Effects of Roof Surface, Slope, and Media Depth. *Journal of Environmental Quality* 34: 1036-1044.

Villarreal E.L. & Bengtsson L. 2005. Response of a Sedum green-roof to individual rain events. *Ecological Engineering* 25: 1-7.

Villarreal E.L. 2005. *Beneficial Use of Stormwater – Opportunities for urban renewal and water conservation*. Doctoral dissertation. Lund Institute of Technology, Department of Water Resources Engineering.

Villarreal E.L. 2004. Runoff detention effect of a *sedum* green-roof. *Nordic Hydrology*: submitted.

Villarreal E.L., Semadeni-Davies A. & Bengtsson L. 2004. Inner city stormwater control using a combination of best management practices. *Ecological Engineering* 22: 279-298.

Wong N.H., Taya S.F., Wonga R., Ongb C.L. & Siab A. 2003. Life Cycle Cost Analysis of Rooftop Gardens in Singapore. *Building and Environment* 38: 499-509.

Wong N.H., Yu C. 2005. Study of green areas and urban heat island in a tropical city. *Habitat International* 29: 547-558.

Personal communication

Lundberg, Louise. Swedish Green Roof Institute. 2005-04-08.

Internet sources

www.gnla.ca. 2004. Goya, N. *Green Roof Policies: Tools for Encouraging Sustainable Design*. http://www.gnla.ca/assets/Policy%20report.pdf, 2005-11-01.

www.greenroofs.com. 2005. Velasquez, L.S. *European airport greenroofs – a potential model for North America*. http://www.greenroofs.com/pdfs/exclusives-european%20-_airport_greenroofs.pdf, 2005-11-01.

www.nrel.gov. MIDC: Measurement and Instrumentation Data Center. 2005. http://www.nrel.gov/midc/solpos/solpos.html, 2005-11-01.

www.oecd.org. 2002. *Shaping the urban environment in the 21st century.* http://www.oecd.org/dataoecd/24/19/1956241.pdf, 2005-11-01.

www.vegtech.se. Veg Tech AB, 2005-10-10.

Appendix A. Sensitivity analysis

Change in Q^*, Q_H and Q_E for changes in albedo (α), emissivity (ε), convection coefficient (h_c) and Q^*/Q_S ratio. Change in %.

			Q^*	Q_H	Q_E	Q^*	Q_H	Q_E
			α -0.05			**α +0.05**		
Sunny	green	100% water	7.37	9.48	6.67	-7.38	-9.48	-6.67
Sunny	green	50% water	7.38	8.43	6.67	-7.38	-8.50	-6.67
Sunny	green	no water	7.30	7.32		-7.36	-7.32	
Sunny	non-green		6.07	6.07		-6.11	-6.11	
Cloudy	green	100% water	7.09	7.38	6.67	-7.10	-7.38	-6.67
Cloudy	green	50% water	7.08	7.33	6.67	-7.09	-7.34	-6.67
Cloudy	green	no water	7.09	7.08		-7.11	-7.07	
Cloudy	non-green		5.70	5.72		-5.72	-5.72	
			ε -0.025			**ε +0.025**		
Sunny	green	100% water	1.85	7.31	0.00	-1.83	-7.08	0.00
Sunny	green	50% water	2.06	5.01	0.00	-2.01	-5.01	0.00
Sunny	green	no water	2.87	2.88		-2.84	-2.80	
Sunny	non-green		2.54	2.54		-2.50	-2.51	
Cloudy	green	100% water	4.60	7.65	0.00	-4.54	-7.51	0.00
Cloudy	green	50% water	4.79	6.85	0.00	-4.73	-6.73	0.00
Cloudy	green	no water	5.36	5.43		-5.29	-5.33	
Cloudy	non-green		4.46	4.55		-4.44	-4.40	
			h_c -2			**h_c +2**		
Sunny	green	100% water	-1.48	-5.72	0.00	1.16	4.54	0.00
Sunny	green	50% water	-2.41	-5.98	0.00	1.91	4.62	0.00
Sunny	green	no water	-6.45	-6.41		5.07	5.08	
Sunny	non-green		-6.42	-6.44		5.04	5.05	
Cloudy	green	100% water	-3.28	-5.26	0.00	2.55	4.15	0.00
Cloudy	green	50% water	-3.77	-5.34	0.00	2.95	4.18	0.00
Cloudy	green	no water	-5.49	-5.49		4.30	4.23	
Cloudy	non-green		-5.42	-5.35		4.18	4.25	
			Q_S/Q^* -0.05			**Q_S/Q^* +0.05**		
Sunny	green	100% water	1.82	-16.33	0.00	-1.78	15.76	0.00
Sunny	green	50% water	1.87	-10.10	0.00	-1.82	9.72	0.00
Sunny	green	no water	2.03	-3.95		-1.97	3.80	
Sunny	non-green		2.03	-3.98		-1.97	3.82	
Cloudy	green	100% water	1.66	-6.97	0.00	-1.64	6.84	0.00
Cloudy	green	50% water	1.70	-6.13	0.00	-1.66	6.01	0.00
Cloudy	green	no water	1.72	-4.23		-1.68	4.14	
Cloudy	non-green		1.68	-4.26		-1.66	4.18	

Appendix B. Monthly simulations

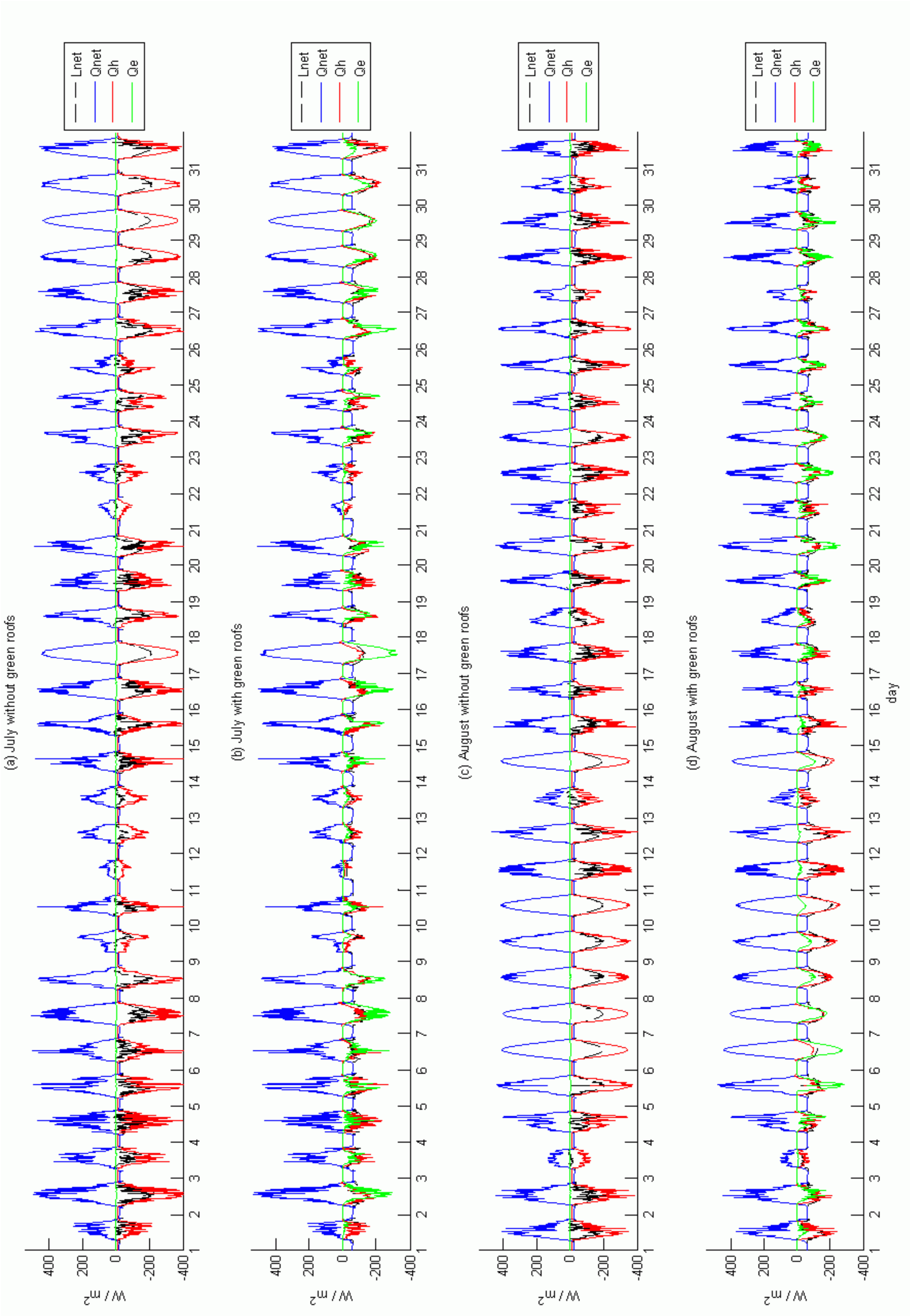

Previous seminar reports

Lunds Universitets Naturgeografiska institution. Seminarieuppsatser. Uppsatserna finns tillgängliga på Naturgeografiska institutionens bibliotek, Sölvegatan 12, 223 62 LUND. Serie startade 1985.

The reports are available at the Geo-Library, Department of Physical Geography, University of Lund, Sölvegatan 12, S-223 62 Lund, Sweden.
Report series started 1985.

79. Ullman, M., (2001): El Niño Southern Oscillation och dess atmosfäriska fjärrpåverkan.
80. Andersson, A., (2001): The wind climate of northwestern Europe in SWECLIM regional climate scenarios.
81. Lalloo, D., (2001): Geografiska informationssystem för studier av polyaromatiska kolväten (PAH) – Undersökning av djupvariation i BO01-området, Västra hamnen, Malmö, samt utveckling av en matematisk formel för beräkning av PAH-koncentrationer från ett kontinuerligt utsläpp.
82. Almqvist, J., Fergéus, J., (2001): GIS-implementation in Sri Lanka.
    Part 1: GIS-applications in Hambantota district Sri Lanka : a case study.
    Part 2: GIS in socio-economic planning : a case study.
83. Berntsson, A., (2001): Modellering av reflektans från ett sockerbetsbestånd med hjälp av en strålningsmodell.
84. Umegård, J., (2001): Arctic aerosol and long-range transport.
85. Rosenberg, R., (2002): Tetratermmodellering och regressionsanalyser mellan topografi, tetraterm och tillväxt hos sitkagran och lärk – en studie i norra Island.
86. Håkansson, J., Kjörling, A., (2002): Uppskattning av mängden kol i trädform – en metodstudie.
87. Arvidsson, H., (2002): Coastal parallel sediment transport on the SE Australian inner shelf – A study of barrier morphodynamics.
88. Bemark, M., (2002): Köphultssjöns tillstånd och omgivningens påverkan.
89. Dahlberg, I., (2002): Rödlistade kärlväxter i Göteborgs innerstad – temporal och rumslig analys av rödlistade kärlväxter i Göteborgs artdataarkiv, ADA.
90. Poussart, J-N., (2002): Verification of Soil Carbon Sequestration - Uncertainties of Assessment Methods.
91. Jakubaschk, C., (2002): Acacia senegal, Soil Organic Carbon and Nitrogen Contents: A Study in North Kordofan, Sudan.
92. Lindqvist, S., (2002): Skattning av kväve i gran med hjälp av fjärranalys.
93. Göthe, A., (2002): Översvämningskartering av Vombs ängar.
94. Lööv, A., (2002): Igenväxning av Köphultasjö – bakomliggande orsaker och processer.
95. Axelsson, H., (2003): Sårbarhetskartering av bekämpningsmedels läckage till grundvattnet – Tillämpat på vattenskyddsområdet Ignaberga-Hässleholm.
96. Hedberg, M., Jönsson, L., (2003): Geografiska Informationssystem på Internet – En webbaserad GIS-applikation med kalknings- och försurningsinformation för Kronobergs län.
97. Svensson, J., (2003): Wind Throw Damages on Forests – Frequency and Associated Pressure Patterns 1961-1990 and in a Future Climate Scenario.
98. Stroh, E., (2003): Analys av fiskrättsförhållandena i Stockholms skärgård i relation till känsliga områden samt fysisk störning.

99. Bäckstrand, K., (2004): The dynamics of non-methane hydrocarbons and other trace gas fluxes on a subarctic mire in northern Sweden.
100. Hahn, K., (2004): Termohalin cirkulation i Nordatlanten.
101. Lina Möllerström (2004): Modelling soil temperature & soil water availability in semi-arid Sudan: validation and testing.
102. Setterby, Y., (2004): Igenväxande hagmarkers förekomst och tillstånd i Västra Götaland.
103. Edlundh, L., (2004): Utveckling av en metodik för att med hjälp av lagerföljdsdata och geografiska informationssystem (GIS) modellera och rekonstruera våtmarker i Skåne.
104. Schubert, P., (2004): Cultivation potential in Hambantota district, Sri Lanka
105. Brage, T., (2004): Kvalitetskontroll av servicedatabasen Sisyla
106. Sjöström., M., (2004): Investigating Vegetation Changes in the African Sahel 1982-2002: A Comparative Analysis Using Landsat, MODIS and AVHRR Remote Sensing Data
107. Danilovic, A., Stenqvist, M., (2004): Naturlig föryngring av skog
108. Materia, S., (2004): Forests acting as a carbon source: analysis of two possible causes for Norunda forest site
109. Hinderson, T., (2004): Analysing environmental change in semi-arid areas in Kordofan, Sudan
110. Andersson, J., (2004): Skånska småvatten nu och då - jämförelse mellan 1940, 1980 och 2000-talet
111. Tränk, L., (2005): Kadmium i skånska vattendrag – en metodstudie i föroreningsmodellering.
112. Nilsson, E., Svensson, A.-K., (2005): Agro-Ecological Assessment of Phonxay District, Luang Phrabang Province, Lao PDR. A Minor Field Study.
113. Svensson, S., (2005): Snowcover dynamics and plant phenology extraction using digital camera images and its relation to CO2 fluxes at Stordalen mire, Northern Sweden.
114. Barth, P. von., (2005): Småvatten då och nu. En förändringsstudie av småvatten och deras kväveretentionsförmåga.
115. Areskoug, M., (2005): Planering av dagsutflykter på Island med nätverkanalys
116. Lund, M., (2005): Winter dynamics of the greenhouse gas exchange in a natural bog.
117. Persson, E., (2005): Effect of leaf optical properties on remote sensing of leaf area index in deciduous forest.
118. Mjöfors, K., (2005): How does elevated atmospheric CO2 concentration affect vegetation productivity?
119. Tollebäck, E.,(2005): Modellering av kväveavskiljningen under fyra år i en anlagd våtmark på Lilla Böslid, Halland
120. Isacsson, C., (2005): Empiriska samband mellan fältdata och satellitdata – för olika bokskogområden i södra Sverige.
121. Bergström, D., Malmros, C., (2005): Finding potential sites for small-scale Hydro Power in Uganda: a step to assist the rural electrification by the use of GIS
122. Magnusson, A., (2005): Kartering av skogsskador hos bok och ek i södra Sverige med hjälp av satellitdata.
123. Levallius, J., (2005): Green roofs on municipal buildings in Lund – Modeling potential environmental benefits.